

SynNotch-CAR T cells overcome challenges of specificity, heterogeneity and persistence in treating xenograft model of glioblastoma

Joseph H. Choe^{1†}, Payal B. Watchmaker^{2†}, Milos S. Simic^{1†}, Ryan D. Gilbert², Aileen W. Li¹, Nira A. Krasnow¹, Kira M. Downey², Wei Yu¹, Diego A. Carrera², Anna Celli³, Juhyun Cho¹, Jessica D. Briones¹, Jason M. Duecker¹, Yitzhar E. Goretsky², Ruth Dannenfelser^{4,5}, Lia Cardarelli^{6,7}, Olga Troyanskaya^{4,5}, Sachdev S. Sidhu^{6,7}, Kole T. Roybal^{1,8-11,*}, Hideho Okada^{2,8,11,*} and Wendell A. Lim^{1,11-12,*}

¹ Cell Design Institute and Department of Cellular & Molecular Pharmacology, University of California, San Francisco, CA 94158, USA.

² Department of Neurological Surgery, University of California, San Francisco, CA 94158, USA.

³ Department of Veterans' Affairs Medical Center, University of California, San Francisco, CA 94158, USA.

⁴ Department of Computer Science, Princeton University, Princeton, NJ 08540, USA.

⁵ Center for Computational Biology, Flatiron Institute, New York, NY 10010, USA.

⁶ Department of Molecular Genetics, University of Toronto, Toronto, Ontario M5S 1A8, Canada.

⁷ Donnelly Centre for Cellular and Biomolecular Research, Banting and Best Department of Medical Research, University of Toronto, M5S 3E1 Toronto, Ontario, Canada.

⁸ Parker Institute for Cancer Immunotherapy, University of California, San Francisco, San Francisco, CA 94158, USA.

⁹ Department of Microbiology and Immunology, University of California, San Francisco, San Francisco, CA 94158, USA.

¹⁰ Chan Zuckerberg Biohub, San Francisco, CA 94158, USA.

¹¹ Helen Diller Cancer Center, University of California, San Francisco, San Francisco, CA 94158, USA.

¹² Howard Hughes Medical Institute, San Francisco, CA 94158, USA.

[†] equal contribution

* co-corresponding authors

Correspondence: kole.roybal@ucsf.edu, hideho.okada@ucsf.edu, wendell.lim@ucsf.edu

One Sentence Summary: synNotch-CAR T cells durably clear glioblastoma xenografts, overcoming dual challenges of antigen heterogeneity and specificity common to solid tumors

ABSTRACT

Treatment of solid cancers with chimeric antigen receptor (CAR) T cells is plagued by the lack of ideal target antigens that are both absolutely tumor-specific and homogeneously expressed. We show that multi-antigen prime-and-kill recognition circuits provide flexibility and precision to overcome these challenges in the context of glioblastoma. A synNotch receptor that recognizes a specific priming antigen, such as the heterogeneous but tumor-specific glioblastoma neoantigen epidermal growth factor receptor splice variant III (EGFRvIII) or the central nervous system (CNS) tissue-specific antigen myelin oligodendrocyte glycoprotein (MOG), can be used to locally induce expression of a CAR. This enables thorough but controlled tumor cell killing by targeting antigens that are homogeneous, but not absolutely tumor specific. Moreover, synNotch regulated CAR expression averts tonic signaling and exhaustion, maintaining a higher fraction of the T cells in a naïve/stem cell memory state. In immunodeficient mice bearing intracerebral patient-derived xenografts (PDX) with heterogeneous expression of EGFRvIII, a single intravenous infusion of EGFRvIII synNotch-CAR T cells demonstrated higher anti-tumor efficacy and T cell durability than conventional constitutively expressed CAR T cells, without off-tumor killing. T cells transduced with a synNotch-CAR circuit primed by the CNS-specific antigen MOG also exhibited precise and potent control of intracerebral PDX without evidence of priming outside of the brain. In summary, by using circuits that integrate recognition of multiple imperfect but complementary antigens, we improve the specificity, completeness, and persistence of T cells directed against glioblastoma, providing a general recognition strategy applicable to other solid tumors.

INTRODUCTION

Although chimeric antigen receptor (CAR) T cells have demonstrated remarkable outcomes in treating hematologic malignancies (*1*), development of effective CAR T therapies for solid cancers remains a challenge, due in large part to the difficulty in identifying optimal target surface antigens. Very few antigens are truly tumor-specific, and the resulting on-target/off-tumor cross-reaction of the engineered T cells with normal tissues can cause lethal toxicities (*2-5*). Conversely, even if antigens with high tumor-specificity are identified, these targets are often heterogeneously expressed, and selective CAR targeting allows for escape of antigen-negative tumor cells (*6*). Thus, there is a general need for new tumor recognition strategies that can navigate the concurrent challenges of specificity and heterogeneity to increase the therapeutic benefit of CAR T cells against solid cancers.

A concrete example of this dual challenge is found in glioblastoma (GBM). The epidermal growth factor receptor splice variant III (EGFRvIII) is a highly GBM-specific neoantigen found in a subset of patients (*7-10*). While this might seem like an ideal tumor-specific antigen target, prior clinical studies targeting GBM with an anti-EGFRvIII CAR showed consistent tumor recurrence. EGFRvIII expression in the tumors is highly heterogeneous, and EGFRvIII⁻ tumor cells can escape and grow, despite effective killing of EGFRvIII⁺ cells by the CAR T cells (*6, 11, 12*). In contrast, alternative glioma-associated target antigens, including Ephrin type A receptor 2 (EphA2) and Interleukin 13 receptor α2 (IL13Rα2), are expressed on the surface of the vast majority of GBM cells (*13-15*), but have imperfect specificity. While they are not expressed in normal CNS tissues, they are expressed in some normal, non-CNS tissues such as the liver, kidney, esophagus and genital organs (<http://www.humanproteomemap.org>). Thus, it is challenging to find a single ideal surface GBM-antigen that is both specific and homogeneous enough to limit the dual challenges of off-target toxicity and incomplete killing.

We therefore proposed that T cells that recognize multi-antigen combinations provide a possible solution to the conundrum of simultaneously optimizing specificity of tumor recognition and completeness of killing. We previously developed “prime-and-kill” circuits in which a synNotch receptor (an engineered receptor that activates a transcriptional output when it recognizes its cognate antigen (*16*)) is primed to induce expression of a CAR directed against a killing antigen (*17, 18*). These synNotch-CAR circuits function as Boolean AND gates, requiring the

recognition of both priming (synNotch) and killing (CAR) antigens. These circuits can also be considered “IF-THEN” circuits, as they execute CAR-directed killing only if first primed by the synNotch ligand. We hypothesized that, by carefully choosing the priming and killing antigens, such multi-antigen circuits could yield hybrid recognition behaviors that could navigate tradeoffs between specificity and heterogeneity.

Here we pursue two such multi-antigen targeting strategies for GBM: priming with either a tumor-specific but heterogeneous neo-antigen (EGFRvIII) or priming with a normal CNS-specific antigen, myelin oligodendrocyte glycoprotein (MOG). SynNotch receptor priming by these antigens was used to locally induce expression of a tandem CAR that recognizes the more homogeneous GBM antigens, EphA2 and IL13Ra2 (13, 19). The expression of EphA2 and IL13Ra2 in other normal tissues makes them non-ideal antigen targets for conventional, single-target CAR T cells. These antigens, however, could serve as effective killing targets, if higher selectivity was restricted by the required priming antigen. Thus, we hypothesized that T cells engineered with prime-and-kill circuits might induce CAR-driven cytotoxicity that was spatially restricted only to the vicinity of priming cells, thereby avoiding off-tumor killing in distant normal tissues that express the killing antigen but that lack the priming antigen.

RESULTS

Prime-and-kill circuit in T cells can overcome antigen heterogeneity by executing trans-killing. Fig. 1 and fig. S1, A and B illustrate our rationale for designing a prime-and-kill circuit in T cells: engineered T cells are first primed by a synNotch receptor that recognizes a cancer-specific but heterogeneous antigen, EGFRvIII, to then induce the expression of a CAR that kills by recognizing a homogenous though imperfectly tumor-specific antigens, such as EphA2 or IL13Ra2 (13, 19). The tandem CAR, which functions as an OR-gate, has an extracellular region containing an α -EphA2 single chain antibody and a IL13 mutein, a variant of IL13 ligand that binds with higher affinity to IL13Ra2 over IL13Ra1 (fig. S1C) (19, 20). The general strategy in this circuit design was to take advantage of the specificity of the priming antigen combined with

the homogeneity of the killing antigens (Fig. 1A), in principle yielding specific and complete tumor killing.

We postulated that priming based on a heterogeneous antigen could yield complete tumor killing, if a T cell primed by one cell could kill a different target cell bearing the killing antigen but lacking the priming antigen, a process we define as trans-killing (Fig. 1B). In contrast, cis-killing would describe priming and killing based on antigens presented on the same cell. To test if synNotch-CAR T cells could execute trans-killing, we first engineered U87 GBM cells to constitutively express the priming antigen EGFRvIII. Native U87 cells do not express EGFRvIII, but they do express both EphA2 and IL13R α 2 killing antigens (11, 12, 21, 22). Thus, we could co-culture U87 EGFRvIII $^+$ cells with U87 EGFRvIII $^-$ cells, and test whether the presence of EGFRvIII $^+$ priming cells was sufficient to induce T cell killing of the EGFRvIII $^-$ target cells. We mixed the U87-EGFRvIII $^+$ and U87-EGFRvIII $^-$ cells in indicated ratios to recapitulate different degrees of heterogeneity observed in patients with GBM then tested if target cell killing by our synNotch-CAR T cells was induced by the presence of priming cells.

We found that CD8 $^+$ T cells engineered with the α -EGFRvIII synNotch- α -EphA2/IL13R α 2 CAR circuit could effectively kill EGFRvIII $^-$ targets cells in vitro, if and only if there were also EGFRvIII $^+$ priming cells present (Fig. 1, C and D; fig. S1, E and F). Priming cells did not need to be present at very high proportions; the presence of as low as 10% priming cells yielded strong killing of EGFRvIII $^-$ target cells, although killing was slightly slower compared to that observed with 50% priming cells ($p=0.0149$ and $p=0.0218$, t test at 48 hours and 72 hours respectively). In contrast, no killing of the EGFRvIII $^-$ target cells was observed in the absence of priming cells. In these assays, we independently tracked the kinetics of killing of the two different tumor cell populations using two different fluorescent labels over 72 hours (movie S1). We also validated effective trans-killing using target cells expressing the model priming and killing antigens, green fluorescent protein (GFP) and CD19, respectively (fig. S2). Altogether, these in vitro studies show that synNotch-CAR T cells can effectively execute trans-killing.

EGFRvIII triggered synNotch-CAR cells kill tumors in vivo only if they contain priming cells. Based on these in vitro data, we next evaluated anti-tumor activities of synNotch-CAR T cells in mice bearing GBM xenografts. First, we confirmed that EGFRvIII-primed T cells could perform

trans-killing of EGFRvIII⁻ GBM cells in vivo, but only in tumors with EGFRvIII⁺ priming cells. As proof of principle, we implanted dual tumors into NOD CRISPR Prkdc Il2r Gamma (NCG) immunodeficient mice. In the brain, we implanted a 1:1 mixture of EGFRvIII⁺ and EGFRvIII⁻ U87 tumor cells. In the flank of the same animals, we implanted EGFRvIII⁻ U87 tumor cells only (Fig. 1E). Here, the flank tumor represents a potentially cross-reactive normal tissue that expresses the killing antigens but not the priming antigen. In contrast, the brain tumor has both priming and killing antigens. On day 6 following the tumor implantation, the mice received intravenous (i.v.) administration of synNotch-CAR T cells or control non-transduced T cells (n=6 per group). All mice treated with control T cells showed tumor growth at both sites and reached the study endpoint with a median survival of 25.5 days. The mice treated with synNotch-CAR T cells, in contrast, demonstrated significant suppression of the intracranial tumor growth compared with that in control mice ($p<0.05$ Fig. 1F). Importantly, however, the mice treated with the synNotch-CAR T cells did not show statistically significant suppression of the flank tumor compared with the control group ($p=0.4$, Fig. 1F). The selective lack of killing in the non-priming flank tumor suggests that the cytotoxic activity of the synNotch-CAR T cells is spatially confined to tumors expressing both priming and killing antigens.

We also performed a systematic comparison of killing of implanted tumors with 0%, 50%, and 100% EGFRvIII⁺ U87 cells (fig. S3). We found that the cohort of mice that received synNotch-CAR T cells did not show any clearance of the 0% EGFRvIII⁺ tumors but showed equally effective tumor clearance of both the 50% and 100% EGFRvIII⁺ tumors ($p<0.001$ and $p<0.001$ respectively, fig. S3B). Thus, in this context, the efficacy of synNotch-CAR T cells is not negatively impacted by EGFRvIII antigen heterogeneity.

EGFRvIII-triggered synNotch-CAR T cells efficiently and durably clear heterogeneous GBM6 PDX tumors better than constitutive CAR T cells. We then sought to evaluate the efficacy of synNotch-CAR T cells in a tumor model which exhibits naturally occurring heterogeneity of EGFRvIII expression. We identified the GBM6 patient-derived xenograft (PDX) tumor as an aggressive GBM model that shows intrinsic EGFRvIII heterogeneity (23) (Fig. 2A). We also confirmed the ability of T cells bearing the α -EGFRvIII synNotch- α -EphA2/IL13Ra2 CAR circuit to detect and kill GBM6 cells in vitro (fig. S4, A and B). We also confirmed that there was a subpopulation of GBM6 cells with undetectable EGFRvIII antigen that were resistant to

killing by the α -EGFRvIII CAR (fig. S4, C and D). Thus, GBM6 represents an ideal tumor model in which to identify circuits that could overcome problems caused by antigen heterogeneity.

We implanted GBM6 tumors in the brains of immunodeficient NCG mice and treated them with T cells bearing the α -EGFRvIII synNotch- α -EphA2/IL13R α 2 CAR circuit. As controls, we treated mice with non-transduced T cells or T cells constitutively expressing either the α -EGFRvIII CAR or α -EphA2/IL13R α 2 tandem CAR (Fig. 2, B to D). All of the mice receiving the untransduced T cells ($n=5$) died of tumor progression by day 43 post-tumor implantation (Fig. 2, C and D). Treatment with the constitutive α -EphA2/IL13R α 2 tandem CAR was largely ineffective. Treatment with the constitutive α -EGFRvIII CAR T cells yielded initial tumor shrinkage, but consistently resulted in recurrence of tumors in all mice (Fig. 2, C and D), recapitulating what has been previously observed in clinical trials deploying this CAR (6). In striking contrast, all of the mice treated with the synNotch-CAR T cells showed complete and long-term remission of the GBM6 tumors. This durable and complete tumor clearance was reproducible (fig. S4E) and was also reflected in significantly increased survival of mice treated with synNotch-CAR T cells ($p=0.0263$ at day 37, Fig. 2D). The synNotch-CAR T cells were also significantly more effective than the constitutive α -EGFRvIII CAR T cells at a lower, suboptimal T cell dosage ($p=0.0017$, Log-rank (Mantel-cox) test Fig. 2E).

To more carefully evaluate the outcome of the different T cell treatments, we performed post-mortem immunofluorescence analysis of mice after 100 days treatment with either the α -EGFRvIII CAR T cells or the synNotch-CAR T cells. Brain slices isolated from 15-day long tumor-bearing mice with no T cell treatment are shown in Fig. 2F (GBM6 tumor cells – yellow; EGFRvIII antigen – red). The constitutive α -EGFRvIII CAR-treated brains showed persistence of GBM6 tumor cells, but no remaining T cells (Fig. 2G, top panel). The remaining GBM6 cells, however, were all negative for EGFRvIII expression, consistent with tumor escape via selective growth of EGFRvIII $^-$ tumor cells. In contrast, the brain sections from mice treated with synNotch-CAR T cells showed complete elimination of GBM6 tumor cells and revealed persistent T cells in the brain parenchyma and meninges (Fig. 2G, bottom panel). In summary, PDX mouse experiments showed that the prime-and-kill circuit could achieve more specific and

complete killing of tumor cells than constitutively-expressed CARs targeted against a single antigen.

Immunofluorescence and intravital imaging show that T cell priming and killing is spatially restricted to GBM tumor. To track the mechanism of synNotch-CAR T cells in more detail, we sectioned brains isolated from GBM6 tumor-bearing mice only 6 days after T cell injection, and evaluated them by immunofluorescence microscopy. In these experiments, GBM6 tumor cells were labelled with the fluorescent protein, mCherry; primed T cells could be detected via a green fluorescent protein (GFP)-tag fused to the induced α -EphA2/IL13R α 2 CAR; apoptotic cells could be detected by staining for cleaved caspase 3 (Fig. 3A). We found that T cell priming and apoptosis spatially overlaid with the GBM6 tumor. Thus, T cell priming and killing were restricted only to the GBM6 tumor, and no collateral killing was observed, even in regions adjacent to the tumor. The same analysis with GBM6 tumor-bearing mice treated with non-transduced T cells, showed no evidence of apoptosis in the tumor or elsewhere (Fig. 3B). Further imaging showed robust infiltration of transferred, hCD45 $^+$ T cells and priming selectively in GBM6 tumor tissue; primed T cells were absent in adjacent normal brain tissue (fig. S5A). Closer examination of these multi-color fluorescent images revealed cytolytic events in the tumor in which apoptotic GBM6 cells are surrounded by primed T cells (fig. S5B).

To more directly visualize T cell priming, we also performed intravital imaging two days after T cell injection (Fig. 3C, movie S2). These time-lapse movies showed a large number of primed T cells only within the tumor, as well as unprimed T cells that became primed as they approached the tumor. Notably, these movies showed that the primed T cells remained stably localized within the tumor over the full course of the 1 hour-long movie, presumably because the T cells were interacting with target cells. Although the primed T cells had dynamic cell processes reaching out to contact neighboring cells, they did not show any sign of rapid trafficking in or out of the tumor. This relatively stable residence of the primed T cells in the tumor may explain the highly specific and localized killing observed with these T cells.

Another feature that is likely to contribute to high spatial targeting specificity is that when the cells leave a microenvironment with priming antigens, the synNotch-induced CAR expression will stop, and the CAR protein will decay. We measured CAR protein decay using a GFP tagged

α -EphA2/IL13R α 2 CAR after removal of a long-term priming cell stimulus (Fig. 3D). We found that CAR levels decayed with a half-life of about 10 hours. This was slightly faster if CAR target cells, such as U87 tumor cells, were present, as these likely accelerated CAR endocytosis. The decay of CAR expression in the observed timeframe likely means that cells that leave the priming environment are not able to sustain a meaningful proliferative and killing response over the course of days to weeks.

SynNotch-induced CAR T cells show a more stem-like phenotype, reduced exhaustion, and improved in vivo persistence compared to constitutive CARs. One of the most surprising findings of these in vivo studies was the improved tumor clearance capacity of the synNotch-CAR T cells compared to the constitutive α -EphA2/IL13R α 2 CAR T cells, since both sets of T cells used the same CAR molecule. Moreover, this difference was only observed in vivo, as the constitutive tandem CAR T cells are highly effective at tumor killing in vitro (Fig. 4A). These puzzling observations suggested that there were additional features of synNotch-CAR circuits that yielded improved anti-tumor activity in vivo.

A general challenge in treating solid cancers with CAR T cells is exhaustion of the T cells, which prevents persistent anti-tumor activity. Recent studies have indicated that tonic signaling by constitutively expressed CARs can play a major role in increasing their susceptibility to exhaustion, leading to poor in vivo T cell persistence (24, 25). We therefore examined the differentiation state of our different types of engineered T cells by flow analysis, and found that all of the α -EGFRvIII synNotch-CAR circuit T cells evaluated in this study contained a higher fraction of cells in a naïve-like state ($CD62L^+ CD45RA^+$, naïve or stem central memory) a phenotype associated with greater in vivo anti-tumor activity (26, 27), compared to the equivalent constitutive CAR T cells (Fig. 4B). We tested different EGFRvIII synNotch-primed circuits, inducing the α -EphA2 CAR, the α -IL13R α 2 CAR, or the tandem α -EphA2/IL13R α 2 CAR, and in all cases, the synNotch-induced version of the CAR yielded a much higher fraction of naïve-like T cells compared to the analogous constitutively expressed CAR (Fig. 4C). Furthermore, this phenotypic improvement seems to be shared by multiple synNotch-CAR circuits (fig. S6).

We evaluated the exhaustion state of the T cells using a panel of exhaustion makers (programmed cell death protein 1: PD1, lymphocyte-activation gene 3: LAG3, T-cell immunoglobulin and mucin-domain containing-3: TIM3) expressed on T cells, both without stimulation or 24 hours after stimulation with GBM target cells (Fig. 4D). In all cases, the constitutively expressed CAR T cells expressed a higher number of exhaustion markers compared to non-transduced T cells or synNotch-CAR T cells. Particularly, upon stimulation, T cells constitutively expressing CAR had significantly more populations expressing two or three exhaustion markers compared with the non-transduced T cells ($p < 0.05$) while synNotch-CAR T cells were not significantly different from the non-transduced T cells ($p=0.999$, $p=0.42$, $p=0.83$ and $p=0.95$ respectively for 0, 1, 2 and 3 exhaustion markers).

Tonic signaling by constitutively expressed CARs has been shown to lead to increased T cell exhaustion (24, 25). Thus, we hypothesized that the synNotch-CAR circuits might show reduced exhaustion and increased stem-like phenotypes because of reduced tonic signaling. Indeed, the synNotch-CAR T cells showed lower tonic signaling than constitutive CAR T cells as measured by CD25 expression in the absence of stimulation ($p=0.037$, Fig. 4E). Additionally, using mass cytometry analyses, synNotch CAR T cells showed higher expression of the stemness marker transcription factor T cell factor 1 (TCF1) and lower expression of the exhaustion marker CD39 compared with constitutive CAR T cells (fig. S7). Thus, synNotch regulation of the CAR appears to prevent tonic signaling and subsequent T cell differentiation and exhaustion.

A more naïve-like and less exhausted phenotype is linked to stronger T cell proliferation and persistence in vivo. We directly investigated T cell persistence in vivo at 6 days after infusion into the tumor-bearing mice, and found abundant synNotch-CAR T cells in the brain. In contrast, we found no surviving constitutive tandem CAR T cells in parallel experiments (Fig. 4F). Together, these findings are consistent with a model in which synNotch-CAR circuits prevent tonic signaling normally observed in constitutively expressed CARs, thereby allowing the T cells to maintain a more naïve, stem-like state less prone to differentiation and exhaustion. Thus, restricting CAR expression locally to the tumor (where priming signals are present) not only increases T cell targeting specificity, but also yields a much more potent and persistent T cell state.

Identification of MOG as a CNS-specific antigen that could be used for tissue-specific priming of inducible CAR T cells. Given the robust trans-killing we observed with EGFRvIII-primed T cells, both in vitro and in vivo, we hypothesized that synNotch-CAR T cells might be capable of priming off of cells near a tumor, even if these priming cells lacked the killing antigen and were not malignant cells. This type of trans-killing could be very useful if, for example, a T cell could be primed by recognizing tissue-specific antigens expressed on non-malignant cells closely associated in space with the tumor (Fig. 5A). For example, in the case of GBM, which rarely metastasize outside of the CNS (28), we might design T cell circuits that are primed by a CNS-specific antigen which then triggers local killing by inducing expression of the tandem CAR against the GBM antigens EphA2 and IL13Ra2. Extensive prior studies indicate that these two killing antigens are not expressed in the normal CNS (29-31). Thus, creating a T cell that restricts its killing to targets that are both in the CNS and EphA2 or IL13Ra2 positive would potentially achieve both high tumor specificity and complete killing. A CNS antigen-primed circuit might thereby provide a solution for treating EGFRvIII-negative GBM.

We bioinformatically identified two candidate brain cell surface proteins, Cadherin 10 (CDH10), a CNS-specific cadherin, and myelin oligodendrocyte glycoprotein (MOG), a surface protein on the myelin sheath of neurons. The predicted tissue expression of these antigens is shown in Fig. 5B and fig. S8. For this study, we focused primarily on using MOG as a priming antigen, as we empirically found it to be more CNS-specific (analysis of CDH10 priming antigen shown in fig. S8). We identified antibody sequences that bind MOG and used them to construct cognate synNotch receptors. We confirmed that these synNotch receptors could be activated by cells expressing either human or mouse MOG protein (Fig. 5C).

We engineered CD8⁺ T cells with the α -MOG synNotch- α -EphA2/IL13Ra2 CAR circuit and co-cultured them with GBM6 target cells in the presence or absence of priming cells (L929 fibroblasts engineered to express MOG). We found that α -MOG synNotch- α -EphA2/IL13Ra2 CAR T cells could effectively kill the GBM6 cells, which do not express MOG, but only in the presence of MOG⁺ priming cells (Fig. 5D). Importantly, we did not observe any off-target killing of the co-cultured priming cells (which lack EphA2 or IL13Ra2 expression), showing that the synNotch-CAR T cells maintained specificity for only killing the CAR antigen-positive tumor cells in the mixture. These in vitro studies demonstrated that the synNotch-CAR T cells could be

safely and efficiently primed for tumor killing by spatially associated non-tumor cells expressing priming antigen.

To test whether the CNS-specific antigen-primed T cells could be effective in vivo, we treated NCG mice implanted with intracranial GBM6 PDX tumors with T cells bearing the α -MOG synNotch- α -EphA2/IL13Ra2 CAR circuit (Fig. 6A). The GBM6 tumor cells do not express MOG, therefore in order for the T cells to kill tumor cells, they must be primed by MOG endogenously expressed in the host mouse CNS. The MOG-primed T cells proved to be highly effective at clearing the GBM6 tumor ($p<0.001$, day 40, Fig. 6B) and increasing mouse survival ($p=0.005$, Fig. 6C) relative to control-treated mice with non-transduced T cells. In mice in which GBM6 tumors were implanted in both the flank and the brain, tumors in the flank were not cleared by the MOG-primed T cells (fig. S8G), consistent with a need for a localized CNS antigen to license the T cells for killing. Similarly, mice treated with T cells bearing the α -CDH10 synNotch- α -EphA2/IL13Ra2 CAR circuit showed effective priming (fig. S8B) and killing of GBM6 both in vitro and in vivo (fig. S8, C to F). However, these synNotch-CAR T cells showed poor discrimination in killing of brain versus flank tumors, suggesting that MOG is superior CNS-specific priming antigen relative to CDH10 (fig. S8G).

Post-mortem immunofluorescence analysis of mice treated with the MOG-primed T cells revealed a high number of T cells in the tumor, with many of these in a primed, CAR-expressing state (Fig. 6D). In tumor-adjacent brain tissue, we observed fewer T cells, but these were also primed and expressing the CAR. In contrast, although many transplanted T cells were found in the spleen, none of them was primed. Similar brain-specific priming of T cells was observed by flow cytometry analysis of brain and spleen samples (fig. S9). These results are consistent with T cell priming throughout the brain, presumably combined with more robust T cell expansion within the tumor as a result of CAR activation and local release of proliferative cytokines.

Given that these T cells are primed by non-malignant cells in the CNS, we wanted to more carefully examine cell killing within the brains of treated animals. We sectioned brain tissue isolated from mice six days after T cell injection and evaluated them by immunofluorescent imaging for both tumor cells and cell apoptosis (Fig. 6, D and E). Cell killing was restricted only within the boundaries of the tumor and did not extend into the normal CNS tissue.

The effectiveness of this CNS-specific antigen-primed circuit represents a novel advance in engineering therapeutic cells. Not only does this circuit represent a possible way to treat EGFRvIII⁺ GBM, but it also represents a general strategy for targeting cell therapies to specific tissues or organs.

Overall, we developed two successful multiple-antigen recognition circuits that rely on either a heterogenous cancer-specific antigen or a CNS tissue-specific antigen to overcome glioblastoma heterogeneity, off-target toxicity and T cell persistence (fig. S10).

DISCUSSION

These results show multiple ways to engineer synNotch-CAR circuits that synergistically combine recognition of complementary antigens that are otherwise imperfect as single antigen targets (fig. S10). One can build circuits that are primed by a highly tumor-specific neoantigen, like EGFRvIII or a tissue-specific antigen, like MOG. Critically, these priming antigens need not be homogeneously expressed on all tumor cells, or be present on any of the tumors cells at all, in the case of tissue-specific priming. Once primed, the T cells can then be programmed to execute complete tumor killing by inducing expression of CARs that target antigens homogenously expressed by tumors, even if these antigens have imperfect specificity individually. By integrating information from multiple antigens and multiple cells, these circuits essentially give improved capability for nuanced recognition of a tumor as a complex tissue, and thus open up many new possibilities for how to recognize and attack tumors in safer and more specific ways. Other related strategies combine CARs and bispecific engagers to integrate multi-antigen combinations (32). The work shown here demonstrates that synNotch-CAR T cells have multiple facets that distinguish them from conventional constitutively expressed single-target CAR T cells, several of which may prove to be highly advantageous in treating other solid cancers beyond GBM (fig. S10).

An inherent dilemma constraining the design of any targeted cancer therapeutic is that increasing specificity to limit off-target toxicity concurrently increases the chance of tumor escape via intrinsic heterogeneity or loss of the molecular target. Here we show that a prime-and-kill circuit

that integrates two or more antigens can be used to navigate this dual optimization problem by relying on highly specific priming antigens, such as the GBM neoantigen EGFRvIII, to then induce the expression of CARs that kill based on a highly homogeneous antigen or set of antigens, such as EphA2 and IL13Ra2. Neither the priming nor killing antigens need to be perfect. EGFRvIII is specific but non-homogeneous, while EphA2 and IL13Ra2 are more homogenous but imperfectly tumor specific. Because their deficiencies are different, these types of antigens can be combined to yield a multi-antigen circuit that is both highly specific and capable of more complete killing. We empirically observe that the EGFRvIII synNotch- α -EphA2/IL13Ra2 CAR T cells are able to effectively and completely clear GBM6 PDX tumors without killing surrounding normal tissue or EphA2 or IL13Ra2-positive cells in other parts of the body that lack co-localized priming antigen.

The ability of these circuits to balance specificity and completeness of killing stems from the ability of the T cells to be primed by one type of cell, and to then be induced to kill CAR antigen-positive target cells within the local environment (trans-killing). Once T cells move away from the environment with priming antigen, they lose CAR expression within hours and are thus unable to sustain a long-term proliferative and killing response, which takes days to weeks. Thus, the T cells are essentially capable of integrating over space to specifically launch potent, large-scale killing only in a microenvironment that contains the right combination of co-localized multiple antigens. Therefore, this targeting strategy is likely to be useful in preventing both toxicity and escape in many other solid tumors, presuming that similar complementary antigen combinations can be identified (33). This represents one of the first anti-tumor strategies that can overcome the intrinsic tradeoff between specificity and limiting evasive escape.

An additional benefit of prime-and-kill circuit in T cells is that the simple act of placing CAR expression under regulated control maintains the T cells in a more naïve-like state that is more durable and less subject to exhaustion. Here, we find that T cells with the constitutive EphA2/IL13Ra2 CAR show no anti-tumor activity in vivo, while T cells with the synNotch-induced version durably clear the GBM tumor. Similar improved anti-tumor activity has been observed for synNotch-CAR T cells targeting other cancers beyond GBM (companion submitted manuscript – Hyrenius-Wittsten et al.), suggesting that these circuits may provide an effective general strategy for treating many solid cancers. These findings are consistent with recent

findings that CAR T cell exhaustion can be limited by intermittent drug-induced repression of CAR signaling (34). In all of these cases, limiting tonic signaling appears to prevent the accumulation of exhausted, terminally differentiated cells. Restricting CAR expression until the T cells enter the tumor thus appears to be a logical strategy for optimizing cell potency and persistence.

Another new finding in this study is that tissue specific antigens, such as MOG, whose expression is restricted to the CNS, can be harnessed as part of a multi-antigen targeted recognition signature for engineered T cell therapies. We find that T cells expressing an α -MOG synNotch receptor can be effectively and specifically primed *in vivo* in the CNS by endogenously expressed MOG. Moreover, if these cells are induced to express the α -EphA2/IL13R α 2 CAR, they only kill CAR antigen-expressing cells in the CNS, and not those implanted outside of the CNS. This priming based on tissue specific antigens is possible because the T cells can then execute trans-killing of tumor cells in the immediate proximity of the non-malignant priming cells. This approach bypasses the need for a cancer-specific priming antigen, and could be employed for GBM that is EGFRvIII-negative. Importantly, this strategy works for the killing antigens EphA2 and IL13R α 2 because these antigens are not normally expressed in the brain, except in the case of tumors (29-31).

The ability to harness normal tissue antigens as part of a multi-antigen targeting signature adds a powerful new way to target cell-based therapies. For example, CNS-specific targeting could be used to more effectively target other CNS tumors or CNS metastases. CNS-targeted cells could also be used to treat other types of CNS diseases beyond cancer, including neuroinflammation or neurodegeneration. Moreover, it is possible that identification of other highly tissue-specific antigens together with more sophisticated circuits (35) could lead to improved targeting of engineered cells to tissues and organs beyond the CNS.

We recognize several limitation of our present study. First, our strategy to design optimal multi-antigen recognition circuits is based on available gene expression data, both for tumors and normal tissues, and this data is not complete and limited in resolution (for example, not all tissues have been analyzed, most is bulk tissue expression rather than single cell, and most is

focused on mRNA levels rather than protein levels). The process of choosing optimal tissue specific priming antigens as well as the best killing antigens for any cancer will improve as better genomic data becomes available. Second, use of immunocompromised mice bearing human GBM and T cells limits our ability to fully characterize the interaction between synNotch-CAR T cells and the native GBM microenvironment. Syngeneic mouse models could help address this, although, ultimately, implementation of a carefully designed phase I clinical trial will be required to evaluate the safety and efficacy of our strategies in human patients.

Here, we have engineered combinatorial recognition T cells that harness existing CAR targets that have previously been clinically shown to be imperfect. We show that by linking these multiple imperfect targets into an integrated multi-antigen recognition T cell, we can generate next-generation T cell therapies that outperform traditional CAR T cells in preclinical models. We are hopeful that similar strategies can be applied to find new cell treatments for other challenging solid cancers.

MATERIALS AND METHODS

Study Design

The objective of this study was to evaluate the therapeutic potential of synNotch-CAR T cells, in comparison with constitutively expressed CAR T cells, to overcome antigenic heterogeneity, off-target toxicity and persistence in a mouse model bearing human patient-derived xenograft (PDX) glioblastoma. For in vivo experiments, 6-10 week old NCG mice were used, with five to ten mice per group to ensure statistical power. Animal size sample was determined by power analysis based on preliminary data. Before CAR T cell treatment, mice were randomized on the basis of bioluminescent imaging to ensure similar average tumor sizes across groups. There was no blinding. Survival was evaluated until predetermined Institutional Animal Care and Use Committee approved endpoint was reached. The brain of each euthanized mouse was collected to confirm the absence of tumor. Prior to in vivo experiments, the T cell circuits were tested in vitro using co-cultures assays. Circuits were tested in T cells from multiple donors. Number of repeats is specified in each figure legend.

Construct Design

SynNotch receptors were built by fusing α -EGFRvIII 139 scFv (11), α -MOG M26 scFv (36), or α -CDH10 scFv (Sidhu lab) to mouse Notch1 (NM_008714) minimal regulatory region (res.1427-1752) and Gal4 DBD VP64. All synNotch receptors contain N-terminal CD8a signal peptide (MALPVTALLLPLALLL HAARP) for membrane targeting and α -myc-tag (EQKLISEEDL) or flag-tag (DYKDDDDK) for detecting surface expression with α -myc A647 (cell-signaling #2233) or a-flag A647 (RND systems #IC8529R); see Morsut et al. (16) for synNotch sequence. Receptors were cloned into a modified pHRSIN:CSW vector containing a PGK or SFFV promoter. The pHRSIN:CSW vector was also used to make response element plasmids with five copies of the Gal4 DNA binding domain target sequence (GGAGCACTGTCCTCC GAACG) upstream from a minimal CMV promoter. Response element plasmids also contain a PGK promoter that constitutively drives mCherry or blue fluorescent protein (BFP) expression to easily identify transduced T cells. CARs were built by fusing EphA2 scFv (37), IL13 Mutein [E13K,K105R] (38), or IL13 Mutein [E13K,K105R]-G4Sx4-EphA2 scFv (37, 38) to the hinge region of the human CD8 α chain and transmembrane

and cytoplasmic regions of the human 4-1BB, and CD3z signaling domains. Inducible CAR constructs were cloned into a BamHI site 3' to the Gal4 response elements. CARs were tagged c-terminally with GFP, BFP, myc tag, or flag tag to verify surface expression.

Primary Human T Cell Isolation and Culture

Primary CD4⁺ and CD8⁺ T cells were isolated from donor blood after apheresis by negative selection (STEMCELL Technologies #15062 and #15063). Blood was obtained from Blood Centers of the Pacific, as approved by the UCSF Institutional Review Board. T cells were cryopreserved in RPMI-1640 (UCSF cell culture core) with 20% human AB serum (Valley Biomedical, #HP1022) and 10% dimethyl sulfoxide. After thawing, T cells were cultured in human T cell medium consisting of X-VIVO 15 (Lonza #04-418Q), 5% Human AB serum, and 10 mM neutralized N-acetyl L-Cysteine (Sigma-Aldrich #A9165) supplemented with 30 units/mL interleukin (IL)-2 (NCI BRB Preclinical Repository) for all experiments except for the IncuCyte experiments. IncuCyte experiments were cultured in RPMI-1640 with 5% human AB serum supplemented with 30 units/mL IL-2.

Lentiviral Transduction of Human T Cells

Pantropic vesicular stomatitis virus G VSV-G pseudotyped lentivirus was produced via transfection of Lenti-X 293T cells (Clontech #11131D) with a pHR'SIN:CSW transgene expression vector and the viral packaging plasmids pCMVdR8.91 and pMD2.G using Fugene HD (Promega #E2312). Primary T cells were thawed the same day and, after 24 hours in culture, were stimulated with Human T-Activator CD3/CD28 Dynabeads (Life Technologies #11131D) at a 1:3 cell:bead ratio. At 48 hours, viral supernatant was harvested and, in some assays, concentrated using Lenti-X concentrator (Clontech #631231). Primary T cells were exposed to the lentivirus for 24 hours. At day 4 after T cell stimulation, Dynabeads were removed, and T cells were expanded until day 9, when they were rested and could be used in assays. T cells were sorted with a Beckton Dickinson (BD) FACS ARIA Fusion or Sony SH800S Cell Sorter. AND-gate T cells exhibiting basal CAR expression were gated out during sorting.

Human T Cell Phenotyping

T cells phenotypes were assessed using the following antibodies: PE anti-CD25 (clone BC96, 302606, BioLegend) for T cell activation; PE-Cy7 anti-PD-1 (clone EH12.1, 561272, BD Biosciences), BV785 anti-TIM-3 (clone F38-2E2, 345031 BioLegend) and AF700 anti-LAG-3 (clone 3DS223H, 56-2239-42, Thermo Fisher) for T cell exhaustion; BV605 anti-CD45RA (clone HI100, 304133, BioLegend) and APC-Cy7 anti-CD62L (clone DREG-56, 304813, BioLegend) T cell differentiation state. Briefly, post-transfected T cells were sorted, expanded and rested for about 10 days, then analyzed by flow cytometry. To assess influence of antigen-dependent activation on T cell phenotype, T cells were cocultured E:T 1:1 (50,000:50,000) for 24 hours with target GBM6 cells pre-stained with CellTrace far red (C34564, Thermo Fisher) per manufacturer's instructions to distinguish them from T cells. We used a 1:100 antibody dilution. A total volume of 50 µL per staining reaction was used in staining buffer (phosphate-buffered saline with 2% fetal bovine serum). Samples were incubated at 4 °C for 15 minutes and washed with staining buffer. T cells were analyzed by flow cytometry.

Cell Lines

Cell lines used were K562 myelogenous leukemia cells (ATCC #CCL-243), L929 mouse fibroblast cells (ATCC# CCL-1), U87 MG GBM cells (ATCC #HTB-14), and GBM6 PDX cells (gift of Frank Furnari, Ludwig Institute and UCSD). U87-EGFRvIII-negative luciferase (12) and U87 MG cells were lentivirally transduced to stably express GFP or mCherry, respectively, under control of the spleen focus-forming virus (SFFV) promoter. At 72 hours after transduction, cells were sorted on an Aria Fusion cell sorter (BD Biosciences) on the basis of GFP or mCherry expression and expanded. Cell lines were sorted for expression of the transgenes. U87-luciferase and U87-luciferase-mCherry cells were stably transduced with non-mutated EGFR using a retroviral construct (gift of Matthew Meyerson; Addgene plasmid # 11011) to generate an EGFRvIII-negative cell line that grows at a similar rate as the EGFRvIII-positive U87 cells. GBM6 were lentivirally transduced to stably express both mCherry and firefly luciferase. These cells were cultured in DMEM F12 media, with supplements of epidermal growth factor EGF (20 µg/mL), fibroblast growth factors FGF (20 µg/mL), and heparin (5 µg/mL). K562 cells were lentivirally transduced to stably express surface CDH10 (CDH10 extracellular membrane was fused to the platelet-derived growth factor transmembrane domain). K562sand L929 cells were lentivirally transduced to stably express full length MOG.

In Vitro Stimulation of SynNotch T cells

For in vitro synNotch-CAR T cell and tumor cell co-culture experiments, 1×10^4 tumor cells (either U87 or GBM6) were cultured overnight in a flat bottom 96-well tissue culture plate. The next morning, $1 \times 10^4 - 5 \times 10^4$ T cells were added to the plate and co-cultures were analyzed for 24 to 96 hours for activation and specific lysis of tumor cells. For in vitro synNotch T cell stimulations co-cultured with three different cell populations, an additional 1×10^4 priming cells (either K562 or L929) were added to the initial overnight culture. Flow cytometry was performed using BD LSRII or Attune NxT Flow Cytometer; analysis was performed by FlowJo software (TreeStar).

Assessment of SynNotch-CAR T Cell Cytotoxicity

CD8⁺ synNotch-CAR T cells were stimulated for 24 to 96 hours as described above with target cells expressing the indicated antigens. The degree of specific lysis of target cells was determined by comparing the fraction of target cells alive in the culture compared to treatment with non-transduced T cell controls, unless stated otherwise. Cell death was monitored by shift of target cells out of the side scatter and forward scatter region normally populated by the target cells. Alternatively, cell viability was analyzed using the IncuCyte Zoom system (Essen Bioscience). Tumor cells were plated into a 96-well plate at a density of 1.0×10^4 cells per well in triplicate overnight. T cells were added at the indicated concentrations into each well next day at a final volume of 200 μ l per well. Target cells and T cells were co-cultured as described above. Two fields of view were taken per well every 15 minutes. Mean fluorescence intensity (MFI) was calculated using IncuCyte Zoom software (Essen BioScience) to determine target cell survival. Data were summarized as mean \pm SEM.

Assessment of CAR Expression Decay In Vitro

EGFRvIII synNotch- α -EphA2/IL13Ra2 CAR T cells were cocultured with excess of target GBM6 cells for 60 hours to induce steady-state CAR expression. Primed, CAR-expressing GFP positive cells (α -EphA2/IL13Ra2 CAR is fused to GFP) were sorted, then cultured alone or with U87 tumor cells. GFP fusion reporter was monitored over time by flow analysis as a readout of CAR decay. Data was fit to exponential decay to estimate the half-life of CAR expression.

In Vivo Mouse Experiments

All mouse experiments were conducted according to Institutional Animal Care and Use Committee (IACUC)-approved protocols. For orthotopic heterogeneous model with U87 tumors, a mixture of 1.5×10^4 U87-luc-EGFRvIII-positive-mCherry cells and 1.5×10^4 U87-luc-EGFRvIII-negative GFP cells was implanted intracranially into 6- to 10-week-old female NCG mice (Charles River), with 6-10 mice per group. For homogeneous U87-luc-GFP-EGFRvIII-positive model, 3×10^4 cells were injected into the brains of NCG mice. For orthotopic heterogeneous model with GBM6, 1.0×10^5 GBM6-luc-mCherry cells were implanted intracranially into 6- to 8-week-old female NCG mice with 5-10 mice per group. Following anesthesia with 1.5% isofluorane, stereotactic surgery for tumor cell implantation (injection volume: 2 μ l) was performed with the coordination of the injection site at 2 mm right and 1 mm anterior to the bregma and 3 mm into the brain. Before and for three days after surgery, mice were treated with an analgesic (Meloxicam and Buprenorphine) and monitored for adverse symptoms in accordance with the IACUC. In the subcutaneous model, NCG mice were injected with either 1.0×10^6 U87-Luc-mcherry⁺ or 1.2×10^5 GBM6-luc-mcherry cells subcutaneously in 100 μ l of HBSS on day 0. Tumor progression was evaluated by luminescence emission on Xenogen IVIS Spectrum after intraperitoneal injection of 1.5mg D-luciferin (GoldBio, injection volume 100 μ l). Prior to treatment, mice were randomized such that initial tumor burden in control and treatment groups were equivalent. Mice were treated with 6.0×10^6 engineered or non-transduced T cells intravenously via tail vein in 100 μ l of phosphate buffered saline (PBS). Survival was evaluated over time until predetermined IACUC-approved endpoint (hunching, neurological impairments such as circling, ataxia, paralysis, limping, head tilt, balance problems, seizures) was reached (n = 6 to 10 mice per group).

Cranial Window Implantation

8-week-old NCG mice underwent tumor implantation with GBM6 xenograft as described above. 10-12 days post-tumor injection, mice underwent implantation of a cranial window and custom designed titanium head plate (UC Berkeley Physics Machine Shop; design by Kira Poskanzer, PhD) according to the following procedure. The cranial window consisted of a No.1 4mm glass coverslip (Warner Scientific) glued onto a No. 1 3mm glass coverslip with optical adhesive

(Norland 71, Norland Products) and cured with 365nm UV light for 15 minutes. Five hours before surgery, mice were injected once intraperitoneally with dexamethasone (2.8mg/kg). At time of surgery, mice were anesthetized with 1.5-3% isoflurane and secured into a stereotactic frame with ear bars. The head was shaved, an oval flap of skin was removed from the top of the head and skin margins were glued down with bio-compatible cyanoacrylate glue (VetBond, 3M). The titanium headplate was superglued (KrazyGlue) to the skull and secured with dental cement at the end of the surgery (C&B Metabond Kit, Parkell). A 3mm diameter craniotomy was performed using a Foredom micro-drill with 1mm and 0.5mm carbide drill bits (McMaster-Carr). The exposed brain was gently irrigated with ice-cold artificial cerebrospinal fluid (150mM NaCl, 2.5mM KCl, 10mM HEPES, pH 7.3), and the cranial window secured with superglue and dental cement. Mice were provided with heat, fluids, and analgesics during post-surgical recovery in accordance with institutional IACUC regulations. T-cell injections were given 15 days after tumor implantation and imaging performed at 1 day and 2 days after adoptive transfer of T cells.

Two-Photon In Vivo Microscopy

Intravital two-photon images were acquired with a Zeiss LSM 780 NLO equipped with a Ti:Sapphire laser (MaiTai HP, Spectra Physics) tuned to 760 nm (for excitation of tagBFP⁺ synNotch CAR T cells and mCherry⁺ tumor) and 900 nm (for excitation of GFP⁺ synNotch CAR T cells), respectively, and focused through a Zeiss 20× water immersion objective (numeric aperture of 1.0). Before imaging, mice were anesthetized with isoflurane and the head plate was fixed into the head posts of a custom-made moving stage (Thorlabs, UC Berkeley Physics Machine Shop). Anesthesia was maintained at 1% isoflurane through a nose cone, and body temperature was kept stable via a temperature-controlled heating pad. Images of 598 × 598 μm² areas of in vivo tumors were acquired at 512 x 512 pixel resolution for standard images and 1,024 × 1,024 pixel resolution for higher resolution images. Volume images were acquired over a 30- to 200-μm Z range in 5- or 10-μm steps. Time-lapse datasets were acquired either in single planes over time periods up to 45 min, or in combined time + Z series over a 598×598 area (X×Y) with variable Z ranges (Z= 5- to 100um) with 1- to 5um steps. Movies were processed in Zen software for 3D reconstructions.

Immunofluorescence

Mice were euthanized before being perfused transcardially with cold PBS. Brains were then removed and fixed overnight in 4% paraformaldehyde–PBS before being transferred to 30% sucrose and were allowed to sink (1-2 days). Subsequently, brains were embedded in O.C.T. Compound (Tissue-Tek; 4583; Sakura Finetek). Serial 10-mm coronal sections were then cut on freezing microtome and stored at -20 °C. Sections were later thawed, fixed with 10% formalin for 10 mins followed by incubation in blocking buffer (PBS-5% normal donkey serum) for 40 minutes and stained with primary antibodies overnight at 4 °C. Primary antibodies used were: CD45 (D9M8I) XP Rabbit mAb (Cell Signaling Technologies, 1:100), Anti-EGFRvIII, clone DH8.3 (Millipore Sigma, 1:100), EphA2 (D4A2) XP Rabbit mAb (Cell Signaling Technologies, 1:100), Anti-IL13 receptor alpha 2 antibody (Abcam, 1:100), and Cleaved Caspase 3 (Asp175) Rabbit mAb (Cell Signaling Technologies, 1:400).

Secondary antibodies raised in donkey and conjugated with Alexa Fluor 647 were used at 4 °C for two hours to detect primary labeling. Sections were stained with nuclear dye DRAQ7 (Abcam) or DAPI (Thermo Fisher). Images were acquired using either a Zeiss Axio Imager 2 microscope ($\times 20$ magnification) with TissueFAXS scanning software (TissueGnostics) or a Zeiss LSM 780 microscope ($\times 20$ magnification) with Zeiss Zen imaging software. Exposure times and thresholds were kept consistent across samples within imaging sessions. Single color images were used to elucidate the regions for quantification. DAPI was used for nuclear segmentation. Colocalization of CD45 (AF647) and GFP signal with nuclear stain was done to obtain counts for GFP⁺ T cells (Strataquest software).

Assessment of Engineered T cells In Vivo

For all experiments involving phenotyping of adoptively transferred engineered T cells, brain and spleen were harvested following perfusion with cold PBS. Brains were mechanically minced and treated at 37 °C for 30 minutes with digestion mix consisting of Collagenase D (30mg/ml) and DNase (10mg/ml) and Soybean trypsin Inhibitor (20mg/ml). The resulting brain homogenate was resuspended in 70% Percoll (GE Healthcare), overlaid with 30% Percoll, and then centrifuged for 30 minutes at 650 x g. Enriched brain infiltrating T cells were recovered at the 70-30% interface and stained with fluorescently conjugated antibodies against CD3 (5ul, Cat no: 555342, BD Biosciences) and CD45 (5ul, Cat no: 564357, BD Biosciences) for one hour at 4

°C. Prior to staining with antibodies, cells were stained with BD Horizon Fixability Viability Stain 780 (BD Biosciences) to discriminate live from dead cells. Data was collected on an Attune NxT Flow Cytometer and the analysis was performed in FlowJo software (TreeStar).

Statistical Analysis

Statistical significance was determined by specific tests and presented as means ± standard error mean (SEM) or means ± standard deviations (SD) as indicated in the figure legends. A Shapiro-Wilk test was used for data normalcy. To assess significant differences between single measurements of two groups of normally distributed data, unpaired or paired two-tailed Student's t test was used; otherwise, Mann-Whitney U test was applied. To assess significant differences between more than two groups of normally distributed data, we performed one-way ANOVA, followed by post hoc analyses: Comparison against a control group was performed using Dunnet's multiple comparisons test, comparison of selected pairs of datasets was performed using Holm-Sidak's multiple comparisons test, and comparison of all pairs of datasets was performed using Tukey's multiple comparisons test. The Kaplan-Meier estimator was used to generate survival curves, and differences in survival distributions were assessed using Log-Rank test. All p values are provided in the figures or their legends. All statistical analyses were performed with Prism software version 7.0 (GraphPad).

Supplementary Materials

Supplementary Materials and Methods

Fig. S1. Construction and testing of α -EGFRvIII synNotch- α -EphA2/IL13R α 2 CAR T cells against U87 GBM.

Fig. S2. Prime-and-kill circuit in T cells can overcome heterogeneity using a model antigen system in vitro.

Fig. S3. α -EGFRvIII synNotch- α -EphA2/IL13R α 2 CAR T cells mediate effective and localized anti-tumor response against U87 GBM that heterogeneously express EGFRvIII in the brain.

Fig. S4. α -EGFRvIII synNotch- α -EphA2/IL13R α 2 CAR T cells are effective against GBM6 tumor cells in vitro and in vivo.

Fig. S5. Fluorescence imaging of brain slices from NCG mice with implanted GBM6 tumors treated with α -EGFRvIII synNotch- α -EphA2/IL13R α 2 CAR T cells.

Fig. S6. SynNotch-CAR T cells show more naïve-like phenotype compared to comparable constitutively expressed CAR T cells.

Fig. S7. Mass cytometry shows that synNotch-induced circuits yield T cells with increased expression of stemness marker TCF1 and reduced expression of exhaustion marker CD39.

Fig. S8. Construction and testing of α -CDH10 synNotch- α -EphA2/IL13R α 2 CAR T cells.

Fig. S9. Brain-specific synNotch-CAR T cells mediate effective anti-GBM responses.

Fig. S10. Strategies for design of synNotch-CAR T cells to treat glioblastoma.

Movie S1. Real-time killing assays using different heterogeneous mixtures of EGFRvIII⁺ and EGFRvIII⁻ target cells show efficient trans-killing.

Movie S2. Intravital imaging of circuit CAR T cells show dynamic priming within the GBM6 xenograft tumor.

Data File S1. Raw Data.

References

1. C. H. June, M. Sadelain, Chimeric Antigen Receptor Therapy. *N. Engl. J. Med.* **379**, 64–73 (2018).
2. L. A. Johnson, R. A. Morgan, M. E. Dudley, L. Cassard, J. C. Yang, M. S. Hughes, U. S. Kammula, R. E. Royal, R. M. Sherry, J. R. Wunderlich, C.-C. R. Lee, N. P. Restifo, S. L. Schwarz, A. P. Cogdill, R. J. Bishop, H. Kim, C. C. Brewer, S. F. Rudy, C. VanWaes, J. L. Davis, A. Mathur, R. T. Ripley, D. A. Nathan, C. M. Laurencot, S. A. Rosenberg, Gene therapy with human and mouse T-cell receptors mediates cancer regression and targets normal tissues expressing cognate antigen. *Blood*. **114**, 535–546 (2009).
3. M. R. Parkhurst, J. C. Yang, R. C. Langan, M. E. Dudley, D.-A. N. Nathan, S. A. Feldman, J. L. Davis, R. A. Morgan, M. J. Merino, R. M. Sherry, M. S. Hughes, U. S. Kammula, G. Q. Phan, R. M. Lim, S. A. Wank, N. P. Restifo, P. F. Robbins, C. M. Laurencot, S. A. Rosenberg, T cells targeting carcinoembryonic antigen can mediate regression of metastatic colorectal cancer but induce severe transient colitis. *Mol. Ther. J. Am. Soc. Gene Ther.* **19**, 620–626 (2011).
4. R. A. Morgan, N. Chinnasamy, D. Abate-Daga, A. Gros, P. F. Robbins, Z. Zheng, M. E. Dudley, S. A. Feldman, J. C. Yang, R. M. Sherry, G. Q. Phan, M. S. Hughes, U. S. Kammula, A. D. Miller, C. J. Hessman, A. A. Stewart, N. P. Restifo, M. M. Quezado, M. Alimchandani, A. Z. Rosenberg, A. Nath, T. Wang, B. Bielekova, S. C. Wuest, N. Akula, F. J. McMahon, S. Wilde, B. Mosetter, D. J. Schendel, C. M. Laurencot, S. A. Rosenberg, Cancer regression and neurological toxicity following anti-MAGE-A3 TCR gene therapy. *J. Immunother. Hagerstown Md 1997*. **36**, 133–151 (2013).
5. R. A. Morgan, J. C. Yang, M. Kitano, M. E. Dudley, C. M. Laurencot, S. A. Rosenberg, Case report of a serious adverse event following the administration of T cells transduced with a chimeric antigen receptor recognizing ERBB2. *Mol. Ther. J. Am. Soc. Gene Ther.* **18**, 843–851 (2010).
6. D. M. O'Rourke, M. P. Nasrallah, A. Desai, J. J. Melenhorst, K. Mansfield, J. J. D. Morrissette, M. Martinez-Lage, S. Brem, E. Maloney, A. Shen, R. Isaacs, S. Mohan, G.

- Plesa, S. F. Lacey, J.-M. Navenot, Z. Zheng, B. L. Levine, H. Okada, C. H. June, J. L. Brogdon, M. V. Maus, A single dose of peripherally infused EGFRvIII-directed CAR T cells mediates antigen loss and induces adaptive resistance in patients with recurrent glioblastoma. *Sci. Transl. Med.* **9** (2017), doi:10.1126/scitranslmed.aaa0984.
7. D. K. Moscatello, M. Holgado-Madruga, A. K. Godwin, G. Ramirez, G. Gunn, P. W. Zoltick, J. A. Biegel, R. L. Hayes, A. J. Wong, Frequent expression of a mutant epidermal growth factor receptor in multiple human tumors. *Cancer Res.* **55**, 5536–5539 (1995).
 8. C. J. Wikstrand, R. E. McLendon, A. H. Friedman, D. D. Bigner, Cell surface localization and density of the tumor-associated variant of the epidermal growth factor receptor, EGFRvIII. *Cancer Res.* **57**, 4130–4140 (1997).
 9. A. B. Heimberger, R. Hlatky, D. Suki, D. Yang, J. Weinberg, M. Gilbert, R. Sawaya, K. Aldape, Prognostic Effect of Epidermal Growth Factor Receptor and EGFRvIII in Glioblastoma Multiforme Patients. *Clin. Cancer Res.* **11**, 1462–1466 (2005).
 10. A. H. Thorne, C. Zanca, F. Furnari, Epidermal growth factor receptor targeting and challenges in glioblastoma. *Neuro-Oncol.* **18**, 914–918 (2016).
 11. L. A. Johnson, J. Scholler, T. Ohkuri, A. Kosaka, P. R. Patel, S. E. McGettigan, A. K. Nace, T. Dentchev, P. Thekkat, A. Loew, A. C. Boesteanu, A. P. Cogdill, T. Chen, J. A. Fraietta, C. C. Kloss, A. D. Posey, B. Engels, R. Singh, T. Ezell, N. Idamakanti, M. H. Ramones, N. Li, L. Zhou, G. Plesa, J. T. Seykora, H. Okada, C. H. June, J. L. Brogdon, M. V. Maus, Rational development and characterization of humanized anti-EGFR variant III chimeric antigen receptor T cells for glioblastoma. *Sci. Transl. Med.* **7**, 275ra22 (2015).
 12. M. Ohno, T. Ohkuri, A. Kosaka, K. Tanahashi, C. H. June, A. Natsume, H. Okada, Expression of miR-17-92 enhances anti-tumor activity of T-cells transduced with the anti-EGFRvIII chimeric antigen receptor in mice bearing human GBM xenografts. *J. Immunother. Cancer.* **1**, 21 (2013).
 13. K. Bielamowicz, K. Fousek, T. T. Byrd, H. Samaha, M. Mukherjee, N. Aware, M.-F. Wu, J. S. Orange, P. Sumazin, T.-K. Man, S. K. Joseph, M. Hegde, N. Ahmed, Trivalent CAR T

- cells overcome interpatient antigenic variability in glioblastoma. *Neuro-Oncol.* **20**, 506–518 (2018).
14. M. Hegde, A. Corder, K. K. H. Chow, M. Mukherjee, A. Ashoori, Y. Kew, Y. J. Zhang, D. S. Baskin, F. A. Merchant, V. S. Brawley, T. T. Byrd, S. Krebs, M. F. Wu, H. Liu, H. E. Heslop, S. Gottschalk, S. Gottachalk, E. Yvon, N. Ahmed, Combinational targeting offsets antigen escape and enhances effector functions of adoptively transferred T cells in glioblastoma. *Mol. Ther. J. Am. Soc. Gene Ther.* **21**, 2087–2101 (2013).
 15. J. Wykosky, D. M. Gibo, C. Stanton, W. Debinski, EphA2 as a Novel Molecular Marker and Target in Glioblastoma Multiforme. *Mol. Cancer Res.* **3**, 541–551 (2005).
 16. L. Morsut, K. T. Roybal, X. Xiong, R. M. Gordley, S. M. Coyle, M. Thomson, W. A. Lim, Engineering Customized Cell Sensing and Response Behaviors Using Synthetic Notch Receptors. *Cell.* **164**, 780–791 (2016).
 17. K. T. Roybal, L. J. Rupp, L. Morsut, W. J. Walker, K. A. McNally, J. S. Park, W. A. Lim, Precision Tumor Recognition by T Cells With Combinatorial Antigen-Sensing Circuits. *Cell.* **164**, 770–779 (2016).
 18. S. Srivastava, A. I. Salter, D. Liggitt, S. Yechan-Gunja, M. Sarvothama, K. Cooper, K. S. Smythe, J. A. Dudakov, R. H. Pierce, C. Rader, S. R. Riddell, Logic-Gated ROR1 Chimeric Antigen Receptor Expression Rescues T Cell-Mediated Toxicity to Normal Tissues and Enables Selective Tumor Targeting. *Cancer Cell.* **35**, 489-503.e8 (2019).
 19. E. Zah, M.-Y. Lin, A. Silva-Benedict, M. C. Jensen, Y. Y. Chen, T Cells Expressing CD19/CD20 Bispecific Chimeric Antigen Receptors Prevent Antigen Escape by Malignant B Cells. *Cancer Immunol. Res.* **4**, 498–508 (2016).
 20. K. S. Kahlon, C. Brown, L. J. N. Cooper, A. Raubitschek, S. J. Forman, M. C. Jensen, Specific recognition and killing of glioblastoma multiforme by interleukin 13-zetakine redirected cytolytic T cells. *Cancer Res.* **64**, 9160–9166 (2004).
 21. K. K. H. Chow, S. Naik, S. Kakarla, V. S. Brawley, D. R. Shaffer, Z. Yi, N. Rainusso, M.-F. Wu, H. Liu, Y. Kew, R. G. Grossman, S. Powell, D. Lee, N. Ahmed, S. Gottschalk, T cells

- redirected to EphA2 for the immunotherapy of glioblastoma. *Mol. Ther. J. Am. Soc. Gene Ther.* **21**, 629–637 (2013).
22. G. Krenciute, S. Krebs, D. Torres, M.-F. Wu, H. Liu, G. Dotti, X.-N. Li, M. S. Lesniak, I. V. Balyasnikova, S. Gottschalk, Characterization and Functional Analysis of scFv-based Chimeric Antigen Receptors to Redirect T Cells to IL13R α 2-positive Glioma. *Mol. Ther. J. Am. Soc. Gene Ther.* **24**, 354–363 (2016).
23. D. A. Nathanson, B. Gini, J. Mottahedeh, K. Visnyei, T. Koga, G. Gomez, A. Eskin, K. Hwang, J. Wang, K. Masui, A. Paucar, H. Yang, M. Ohashi, S. Zhu, J. Wykosky, R. Reed, S. F. Nelson, T. F. Cloughesy, C. D. James, P. N. Rao, H. I. Kornblum, J. R. Heath, W. K. Cavenee, F. B. Furnari, P. S. Mischel, Targeted Therapy Resistance Mediated by Dynamic Regulation of Extrachromosomal Mutant EGFR DNA. *Science*. **343**, 72–76 (2014).
24. R. C. Lynn, E. W. Weber, E. Sotillo, D. Gennert, P. Xu, Z. Good, H. Anbunathan, J. Lattin, R. Jones, V. Tieu, S. Nagaraja, J. Granja, C. F. A. de Bourcy, R. Majzner, A. T. Satpathy, S. R. Quake, M. Monje, H. Y. Chang, C. L. Mackall, c-Jun overexpression in CAR T cells induces exhaustion resistance. *Nature*. **576**, 293–300 (2019).
25. A. H. Long, W. M. Haso, J. F. Shern, K. M. Wanhaninen, M. Murgai, M. Ingaramo, J. P. Smith, A. J. Walker, M. E. Kohler, V. R. Venkateshwara, R. N. Kaplan, G. H. Patterson, T. J. Fry, R. J. Orentas, C. L. Mackall, 4-1BB costimulation ameliorates T cell exhaustion induced by tonic signaling of chimeric antigen receptors. *Nat. Med.* **21**, 581–590 (2015).
26. D. Sommermeyer, M. Hudecek, P. L. Kosasih, T. Gogishvili, D. G. Maloney, C. J. Turtle, S. R. Riddell, Chimeric antigen receptor-modified T cells derived from defined CD8+ and CD4+ subsets confer superior antitumor reactivity in vivo. *Leukemia*. **30**, 492–500 (2016).
27. L. Gattinoni, E. Lugli, Y. Ji, Z. Pos, C. M. Paulos, M. F. Quigley, J. R. Almeida, E. Gostick, Z. Yu, C. Carpenito, E. Wang, D. C. Douek, D. A. Price, C. H. June, F. M. Marincola, M. Roederer, N. P. Restifo, A human memory T cell subset with stem cell-like properties. *Nat. Med.* **17**, 1290–1297 (2011).

28. M. Awan, S. Liu, A. Sahgal, S. Das, S. T. Chao, E. L. Chang, J. P. S. Knisely, K. Redmond, J. W. Sohn, M. Machtay, A. E. Sloan, D. B. Mansur, L. R. Rogers, S. S. Lo, Extra-CNS metastasis from glioblastoma: a rare clinical entity. *Expert Rev. Anticancer Ther.* **15**, 545–552 (2015).
29. J. Wykosky, D. M. Gibo, C. Stanton, W. Debinski, EphA2 as a novel molecular marker and target in glioblastoma multiforme. *Mol. Cancer Res. MCR.* **3**, 541–551 (2005).
30. W. Debinski, N. I. Obiri, S. K. Powers, I. Pastan, R. K. Puri, Human glioma cells overexpress receptors for interleukin 13 and are extremely sensitive to a novel chimeric protein composed of interleukin 13 and pseudomonas exotoxin. *Clin. Cancer Res. Off. J. Am. Assoc. Cancer Res.* **1**, 1253–1258 (1995).
31. J. Wykosky, D. M. Gibo, C. Stanton, W. Debinski, Interleukin-13 receptor alpha 2, EphA2, and Fos-related antigen 1 as molecular denominators of high-grade astrocytomas and specific targets for combinatorial therapy. *Clin. Cancer Res. Off. J. Am. Assoc. Cancer Res.* **14**, 199–208 (2008).
32. B. D. Choi, X. Yu, A. P. Castano, A. A. Bouffard, A. Schmidts, R. C. Larson, S. R. Bailey, A. C. Boroughs, M. J. Frigault, M. B. Leick, I. Scarfò, C. L. Cetrulo, S. Demehri, B. V. Nahed, D. P. Cahill, H. Wakimoto, W. T. Curry, B. S. Carter, M. V. Maus, CAR-T cells secreting BiTEs circumvent antigen escape without detectable toxicity. *Nat. Biotechnol.* **37**, 1049–1058 (2019).
33. R. Dannenfelser, G. M. Allen, B. VanderSluis, A. K. Koegel, S. Levinson, S. R. Stark, V. Yao, A. Tadych, O. G. Troyanskaya, W. A. Lim, Discriminatory Power of Combinatorial Antigen Recognition in Cancer T Cell Therapies. *Cell Syst.* **11**, 215-228.e5 (2020).
34. E. W. Weber, R. C. Lynn, E. Sotillo, J. Lattin, P. Xu, C. L. Mackall, Pharmacologic control of CAR-T cell function using dasatinib. *Blood Adv.* **3**, 711–717 (2019).
35. J. Z. Williams, G. M. Allen, D. Shah, I. S. Sterin, K. H. Kim, V. P. Garcia, G. E. Shavey, W. Yu, C. Puig-Saus, J. Tsoi, A. Ribas, K. T. Roybal, W. A. Lim, Precise T cell recognition

- programs designed by transcriptionally linking multiple receptors. *Science*. **370**, 1099–1104 (2020).
36. H.-C. von Büdingen, S. L. Hauser, A. Fuhrmann, C. B. Nabavi, J. I. Lee, C. P. Genain, Molecular characterization of antibody specificities against myelin/oligodendrocyte glycoprotein in autoimmune demyelination. *Proc. Natl. Acad. Sci.* **99**, 8207–8212 (2002).
 37. Y. Goldgur, P. Susi, E. Karellehto, H. Sanmark, U. Lamminmäki, E. Oricchio, H.-G. Wendel, D. B. Nikolov, J. P. Himanen, Generation and characterization of a single-chain anti-EphA2 antibody. *Growth Factors Chur Switz.* **32**, 214–222 (2014).
 38. S. Krebs, K. K. H. Chow, Z. Yi, T. Rodriguez-Cruz, M. Hegde, C. Gerken, N. Ahmed, S. Gottschalk, T cells redirected to interleukin-13R α 2 with interleukin-13 mutein--chimeric antigen receptors have anti-glioma activity but also recognize interleukin-13R α 1. *Cytotherapy*. **16**, 1121–1131 (2014).

ACKNOWLEDGEMENTS

We thank J. Williams, R. Hernandez-Lopez, V. Tieu, N. Blizzard, J. Shon, H. Ogino, M. Shahin and members of the W.A.L. lab and H.O. lab for assistance, advice, and helpful discussions. This study was supported in part by HDFCCC Laboratory for Cell Analysis Shared Resource Facility through a grant from NIH (P30CA082103).

FUNDING

This work was supported by grants from the NIH - U54CA244438 (W.A.L.), R01 CA196277 (W.A.L.), and 1R35 NS105068 (H.O), the Howard Hughes Medical Institute (W.A.L.), UCSF Glioblastoma Precision Medicine Program (W.A.L. and H.O) and Parker Institute for Cancer Immunotherapy (W.A.L. and H.O).

AUTHOR CONTRIBUTIONS

Conceptualization, J.H.C., P.B.W., M.S.S., K.T.R., H.O., and W.A.L.; Brain-Priming Circuits, M.S.S. and J.H.C.; Formal Analysis, J.H.C., P.B.W. and M.S.S.; Funding Acquisition, H.O. and W.A.L.; Investigation, J.H.C., P.B.W., M.S.S., R.D.G., D.A.C, W.Y., K.M.D., N.A.K., A.W.L, R.D., J.M.D., Y.E.G., J.C., and J.D.B; Methodology, J.H.C., P.B.W. and M.S.S.; Project Administration, J.H.C., P.B.W., M.S.S., K.T.R., H.O., and W.A.L. Resources, S.S.; Supervision, K.T.R., H.O., and W.A.L.; Visualization, J.H.C., P.B.W., M.S.S. and W.A.L.; Writing – original draft, J.H.C., P.B.W., K.T.R., H.O., and W.A.L.; Writing – review and editing, J.H.C., P.B.W., M.S.S., R.D.G., K.T.R., H.O., and W.A.L.

Conflicts of Interest

W.A.L. is on the Scientific Advisory Board for Allogene Therapeutics and is a shareholder of Gilead Sciences and Intellia Therapeutics. H.O. is on the on the Scientific Advisory Board for Neuvogen and Eureka Therapeutics. K.T.R. is a co-founder or Arsenal Biosciences.

W.A.L., H.O., P.B.W. and J.H.C. are inventors on the following relevant patent/patent applications held/submitted by UCSF: Trans-Antigen Targeting in Heterogeneous Cancers and Methods of Use Thereof (WO 2019/195576 A1) (2019); Methods of Treating EGFRvIII-Expressing Glioblastomas (WO2019/195586 A1; .US 62/654,012) (2019); Methods of treating

glioblastomas (WO2019195596A1) (2019); W.A.L., H.O., P.B.W., J.H.C and M.S.S. are inventors on the following relevant patent/patent applications held/submitted by UCSF: Use of MOG for priming a treatment for glioblastoma (US 62/980,882) (2020) and 5) Use of brain-specific antigens to home, block and deliver cell-based treatments to the brain (US 62/980,885) (2020). H.O. is an inventor on patent Treatment of cancer using humanized anti-EGFRvIII chimeric antigen receptor US20190330356A1 (2019) held by University of Pennsylvania and University of Pittsburgh that covers EGFRvIII-targeting.

Data Availability

All data associated with this study are in the paper or supplementary materials. All reagents will be made available to members of the research community following completion of a materials transfer agreement. Reagent requests should be directed to Wendell Lim (Wendell.lim@ucsf.edu) and copied to Noleine Blizzard (noleine.blizzard@ucsf.edu) and Michael Broeker (Michael.Broeker@ucsf.edu).

FIGURES

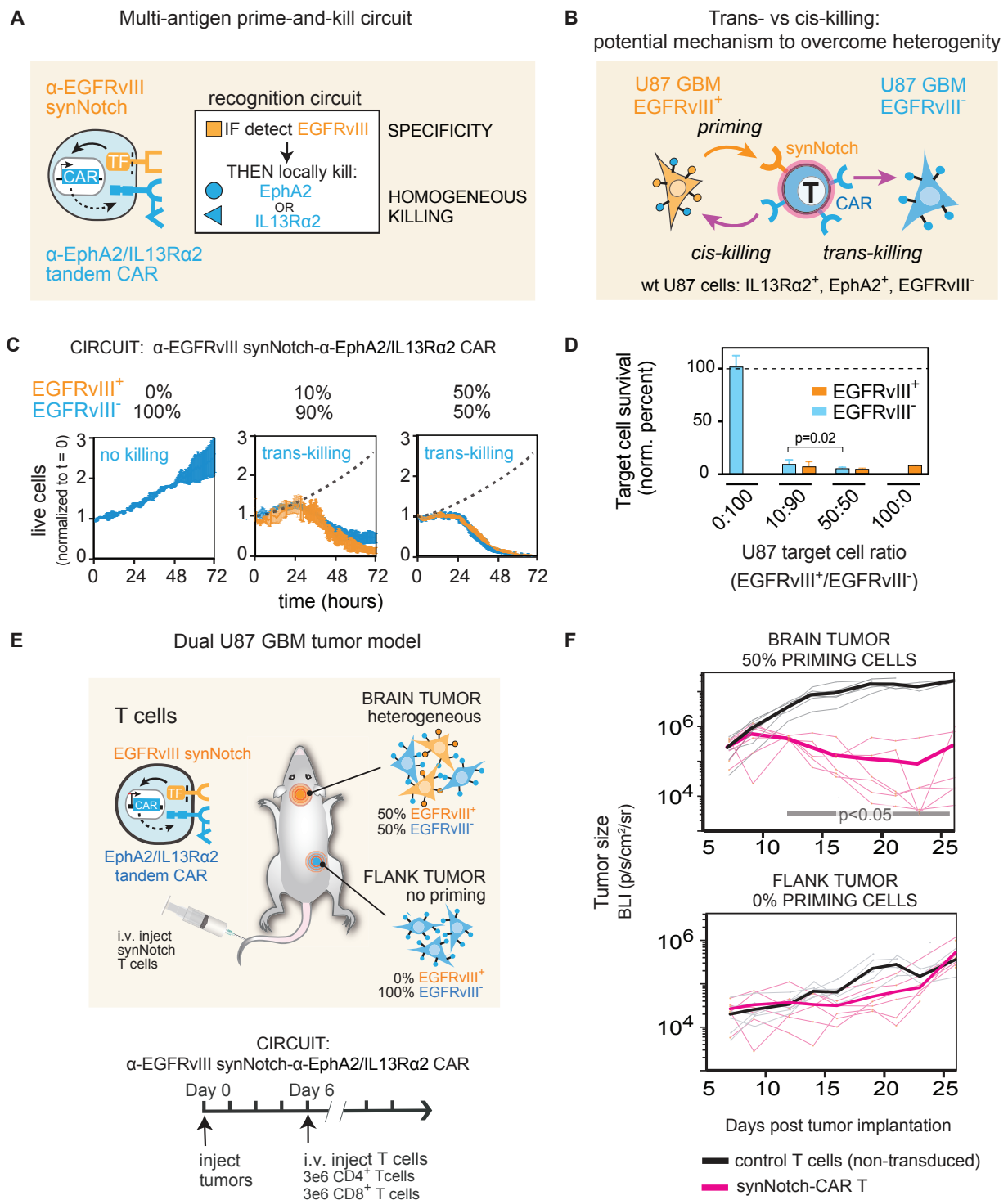


Figure 1. Multi-antigen prime-and-kill circuits in T cells provide a general strategy to overcome antigen heterogeneity while still maintaining high tumor specificity. (A) Design of synNotch-CAR circuit primed by EGFRvIII neoantigen: α-EGFRvIII synNotch receptor induces

expression of tandem α -EphA2/IL13R α 2 CAR (TF: transcription factor). These cells should be activated to kill EphA2 $^+$ or IL13R α 2 $^+$ target cells only if exposed to EGFRvIII $^+$ cells. **(B)** Such T cells could overcome priming antigen heterogeneity if they can execute trans-killing, where priming and killing antigens are expressed on different but neighboring cells. **(C)** Real-time killing assays using heterogeneous mixtures of EGFRvIII $^+$ and EGFRvIII $^-$ target cells show efficient trans-killing. Primary CD8 $^+$ human T cells transduced with α -EGFRvIII synNotch- α -EphA2/IL13R α 2 CAR circuit were cultured with indicated ratios of EGFRvIII $^+$ vs EGFRVIII $^-$ U87 cells, at an E:T ratio of 5:1 and imaged over 3 days using IncuCyte. The EGFRvIII $^+$ cell population (priming cells) is shown in yellow and the EGFRvIII $^-$ cell population (target cells) is shown in blue. The presence of as low as 10% priming cells yielded strong killing of EGFRvIII $^-$ target cells, although killing was slightly slower compared to that observed with 50% priming cells ($p=0.0149$ and $p=0.0218$, t test at 48 hours and 72 hours respectively). The dotted black line shows the growth of 100% target cells as a reference ($n=3$, error bars denote SEM). See movie S1. **(D)** Relative survival of each cell type in experiments from panel C (at 72 hours) is shown. Killing of target cells is efficiently primed by as low as 10% priming cells (EGFRvIII $^+$). No killing is observed in absence of priming cells ($n=3$, error bars denote SD). A t test was used for statistical comparison. **(E)** NCG mice were simultaneously implanted with two GBM tumors, a heterogeneous tumor comprising EGFRvIII $^+$ and EGFRvIII $^-$ U87 cells (1:1 ratio) in the brain, and a homogeneous EGFRvIII $^-$ U87 tumor implanted subcutaneously in the flank. Mice were treated 6 days after tumor implantation with intravenous (i.v.) infusion of 3 million CD4 $^+$ and CD8 $^+$ synNotch-CAR T cells ($n=6$) or control non-transduced T cells ($n=6$). **(F)** Tumor size was measured by luciferase bioluminescence imaging (BLI) over time as the number of photons per second per square centimeter per steradian: p/s/cm 2 /sr. Tumor size curves for individual mice treated with synNotch-CAR T cells shown in light pink; curves for mice treated with non-transduced T cells shown in gray. Thicker lines correspond to geometric means. $p < 0.05$ by Mann Whitney test on day 12 and onwards, while the flank tumor grew at the same rate as in the mice treated with non-transduced T cells.

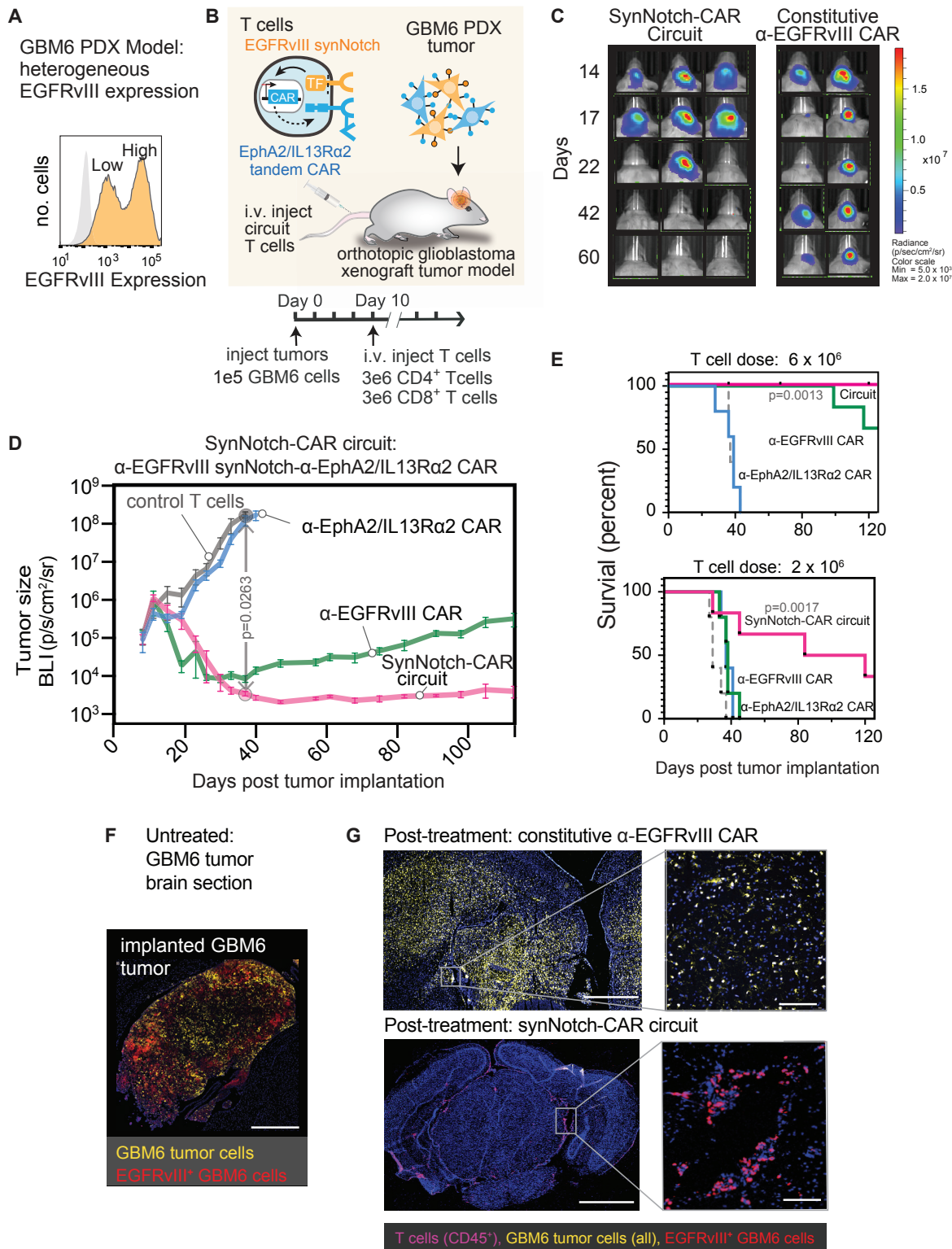


Figure. 2. SynNotch-CAR T cells show improved efficacy and durability compared to individual parental constitutive CARs in clearing heterogeneous GBM6 PDX tumors. (A) Flow cytometry analysis of a patient-derived xenograft (PDX) GBM6 tumor model shows

intrinsic heterogeneity of EGFRvIII expression. **(B)** Timeline for in vivo tumor experiments with GBM6 tumors. GBM6 tumors expressing mCherry and luciferase were orthotopically implanted in brains of NCG mice. Ten days after tumor implantation, mice were infused intravenously (i.v.) with 3 million each of CD4⁺ and CD8⁺ T cells expressing no construct (control) (n=5), α -EGFRvIII synNotch- α -EphA2/IL13R α 2 CAR circuit (n=6), constitutively expressed α -EGFRvIII CAR (n=5), or constitutively expressed α -EphA2/IL13R α 2 tandem CAR (n=5). **(C)** Longitudinal bioluminescence imaging of GBM6 bearing mice treated with α -EGFRvIII synNotch- α -EphA2/IL13R α 2 CAR T cells and conventional α -EGFRvIII CAR T cells is shown. Each column represents one mouse over time. **(D)** Time course of tumor size measured by bioluminescence. p=0.0263, two-way ANOVA followed by a Dunnett's test non-transduced vs synNotch-CAR T cells at day 37. Error bars represent mean \pm SEM of 5-6 individual mice from one experiment. **(E)** Kaplan-Meier survival curves for high (6×10^6 cells) and low dose (2×10^6 cells) treatments. Statistical significance calculated using log-rank Mantel-Cox test. **(F)** Fluorescence microscopy of representative section of untreated GBM6 xenograft tumor, isolated 15 days post tumor implantation, shows heterogeneous expression of EGFRvIII. Scale bar, 500 μ m. **(G)** Top panel: representative fluorescence microscopy of a brain and tumor section isolated 107 days post-treatment with conventional α -EGFRvIII CAR T cells shows presence of tumor but loss of EGFRvIII expression. Bottom panel: representative fluorescence microscopy of a brain section isolated 110 days post treatment with EGFRvIII synNotch- α -EphA2/IL13R α 2 CAR T cells reveals clearance of a GBM6 xenograft tumor and sustained presence of T cells. Scale bar, 1mm (left), 50 μ m (right).

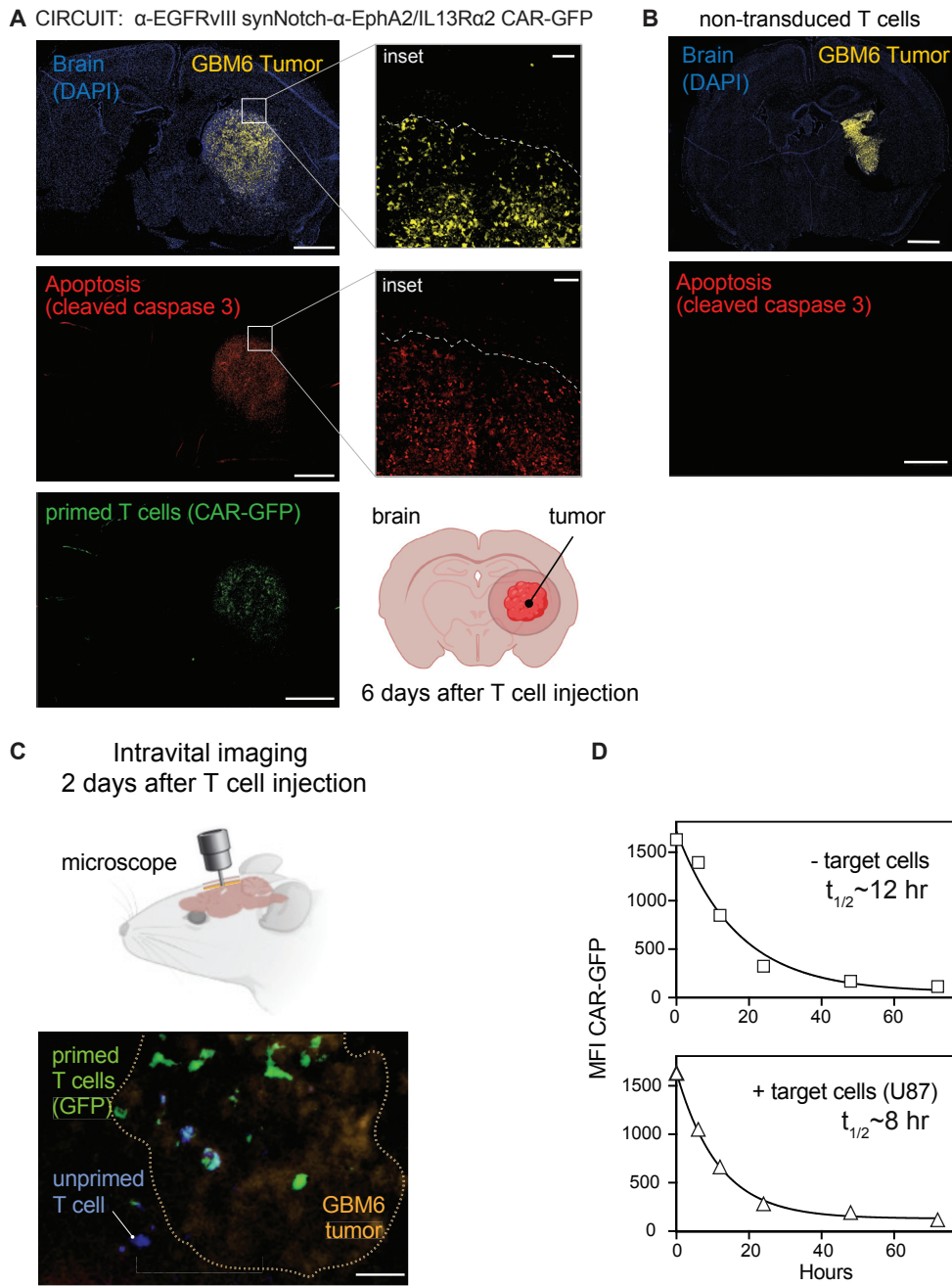


Figure 3. Early timepoint imaging shows that priming and killing of synNotch-CAR T cells are precisely restricted to tumor region. (A) Representative confocal fluorescent microscopy of brain slices from GBM6 tumor-bearing mice isolated at 6 days after infusion with α -EGFRvIII synNotch- α -EphA2/IL13Ra2 CAR T cells reveals primed T cells expressing CAR-GFP only within the tumor bed. Cleaved caspase 3 is also only observed within the tumor. Scale bar, 1mm (left), 100 μ m (right). Overlay of tumor, cleaved caspase 3 and primed GFP T cell is shown in fig. S5B. (B) Representative confocal images of brain slices from GBM6 tumor-bearing mice

isolated at 6 days post treatment with non-transduced T cells. Scale bar, 1mm. **(C)** Intravital two-photon imaging of synNotch-CAR T cells show priming within the GBM6 xenograft tumor. Tumors were implanted at a depth of 3mm below the right frontal cortex and cranial windows were implanted. Scale bar, 400um. See movie S2. **(D)** Half-life of CAR expression decay in synNotch-CAR T cells after removing priming cells. T cells were primed in vitro with GBM6 cells for 60 hours, then isolated by cell sorting. GFP-tagged CAR expression was observed over time. MFI: median fluorescence intensity. Decay experiment was performed in absence (top) or presence (bottom) of target U87 cells lacking priming antigen. Exponential decay fit was used to determine the CAR half-life. Decay curves depict one representative of 4 different donors.

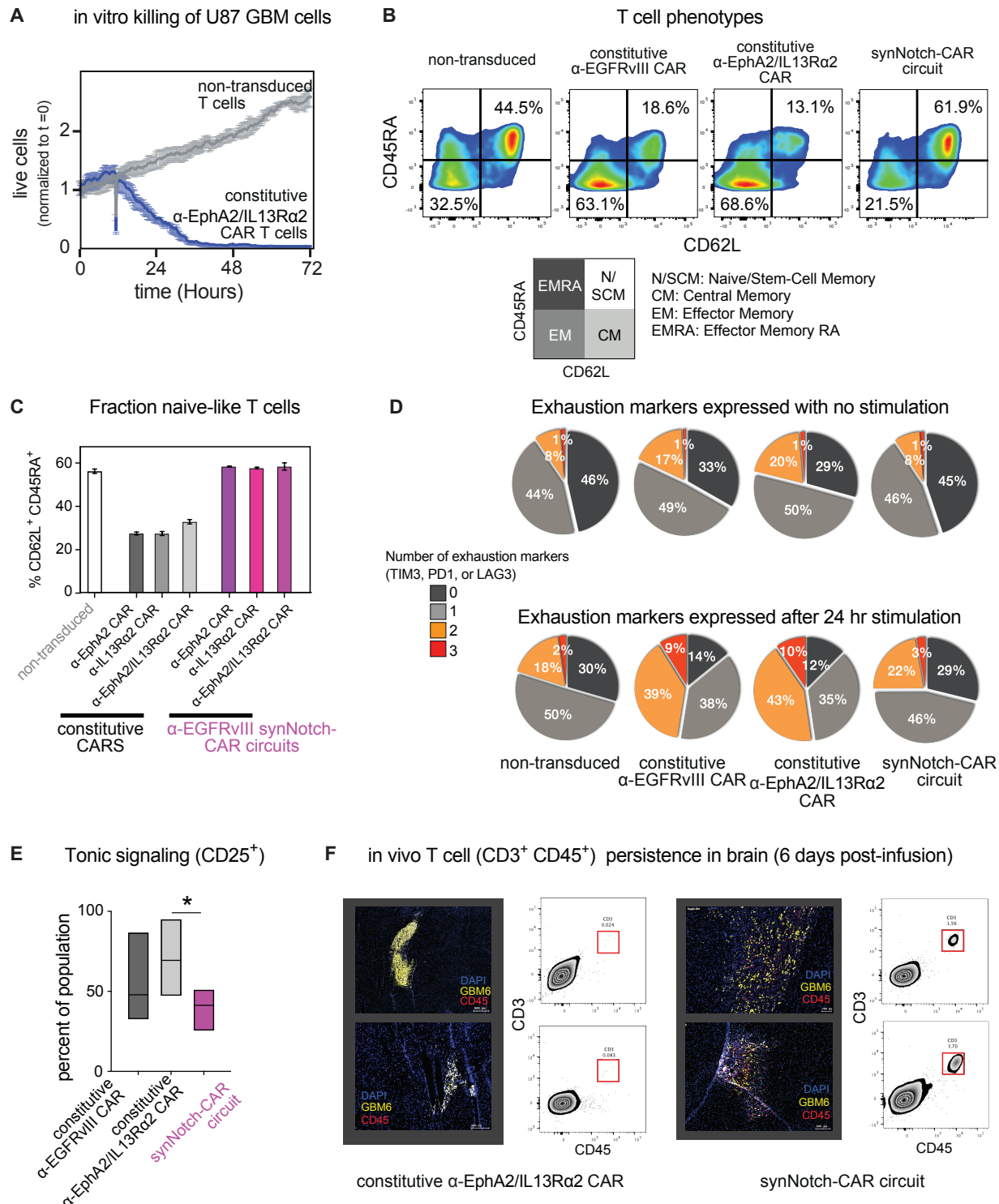


Figure 4. SynNotch-CAR T cells show enhanced naïve/stem-cell memory phenotype, reduced exhaustion and improved persistence in vivo. (A) In vitro killing by T cells constitutively expressing α -EphA2/IL13Ra2 tandem CAR (relative to non-transduced control). (B) Flow cytometry plots distinguishing naïve-like cells ($CD45RA^+CD62L^+$), central memory

cells ($CD45RA^-CD62L^+$), effector memory cells ($CD45RA^-CD62L^-$), and effector memory RA cells ($CD45RA^+CD62L^-$) (representative of 3 experiments from different donors). Percentages of cells in the naïve/memory stem cell state and effector memory state are highlighted. T cells were rested for 10 days in vitro after transfection before phenotypic analysis. **(C)** Percentage of $CD62L^+CD45RA^+$ T cells in indicated CAR T cells and synNotch-CAR T cells ($n=3$ per group). **(D)** Expression of exhaustion markers by indicated CAR and synNotch-CAR T cells, both without and with stimulation by target cells. Pie chart shows percentage of cells that express 0, 1, 2, or 3 exhaustion markers (PD1, LAG3, or TIM3), average of 3 different donors. **(E)** Tonic signaling in constitutive vs α -EGFRvIII-synNotch induced α -EphA2/IL13R α 2 CAR T cells, measured by percent $CD25^+$ cells (one-way ANOVA followed by a Dunnett's test, $p < 0.05$, $n = 5$ different donors). Boxes represent min to max with median center line. **(F)** SynNotch-CAR T cells show improved persistence in vivo compared to constitutive CAR T cells. GBM6 tumor-bearing mice were euthanized six days after infusion of either the constitutive tandem CAR T cells (left panels) or α -EGFRvIII synNotch- α -EphA2/IL13R α 2 CAR T cells (right panels). Representative confocal fluorescent microscopy of brain slices and single-cell suspensions of tumor-bearing brain show few T cells ($CD3^+CD45^+$) in constitutive CAR T cell-treated tumors. In contrast, mice treated with synNotch-CAR T cells reveal high number of T cells in tumors.

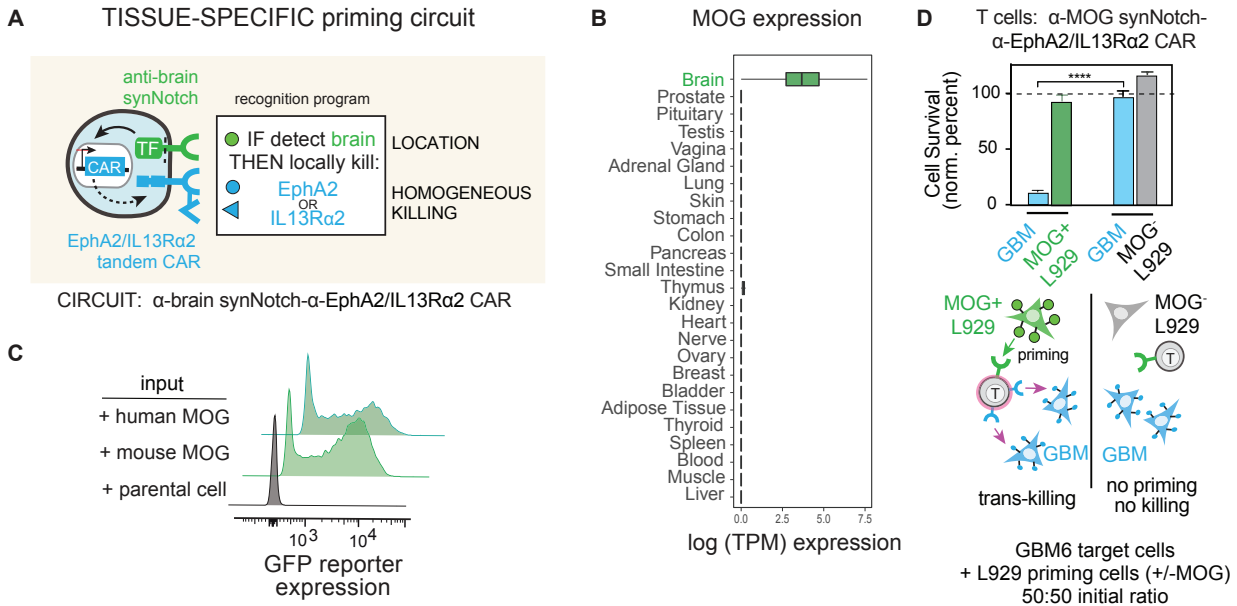


Figure 5. Design of brain antigen-primed synNotch-CAR circuit to target GBM. (A)
 “Tissue-specific priming” circuit is designed to restrict killing only to the brain, preventing damage to normal, non-brain tissues that express killing antigens, EphA2 and IL13Ra2. In principle, this circuit should selectively identify GBM cells as the only brain-localized cells that are EphA2⁺ or IL13Ra2⁺. **(B)** Box and whisker plots showing tissue specific expression of MOG across a subset of tissue samples in GTEx v7. Units shown are log scaled normalized RNAseq counts (Transcripts Per Million) taken from GTEx portal v7 (<https://gtexportal.org/>). **(C)** Primary CD8⁺ T cells expressing α -MOG synNotch and GFP reporter were co-cultured with either parental K562 cells or K562 cells expressing mouse or human MOG. Flow cytometry histograms show induction of GFP reporter only in the presence of MOG⁺ K562 cells (representative of 3 experiments). **(D)** Primary CD8⁺ T cells transduced with α -MOG synNotch- α -EphA2/IL13Ra2 CAR circuit were co-cultured with GBM6 target cells and L929 priming cells either expressing or not expressing mouse MOG. Relative cell survival of both target GBM and priming L929 cells was tracked over 72 hours. (n=3, error bars indicate SD). **** p < 0.0001; t test compared to those co-cultured with MOG⁻ L929 cells. The cell population ratio was 1:1:1, 1x 10⁴ cells each. No significant killing of the L929 priming cell population was observed in either experiment.

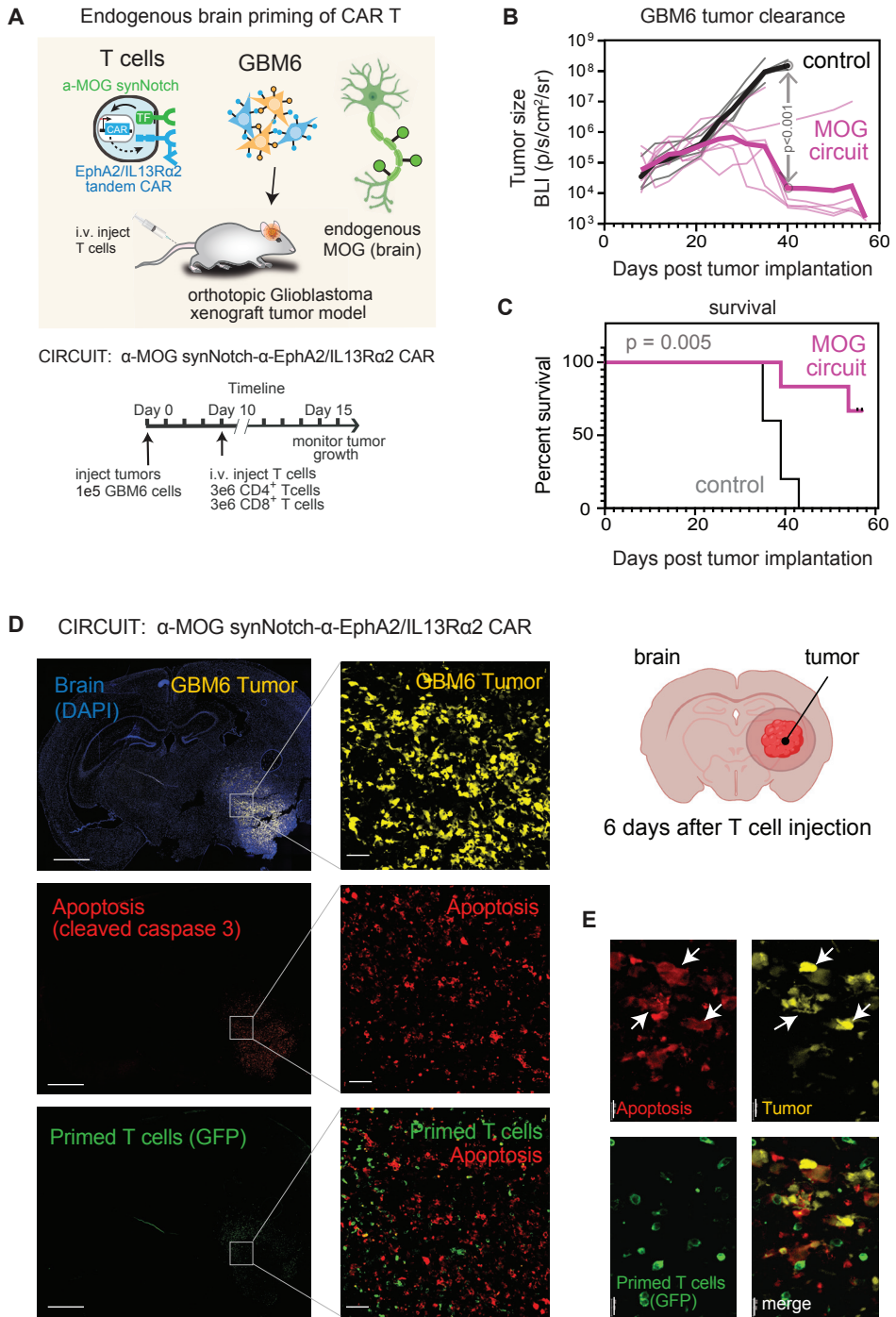


Figure 6. Tissue-specific priming of synNotch-CAR T cells by brain-specific antigen MOG induces effective killing of GBM6 brain tumors *in vivo*. (A) GBM6 tumor cells were stereotactically implanted into brains of NCG mice. GBM6 cells were engineered to express mCherry and luciferase to allow for tracking of tumor size. Ten days after tumor implantation, mice were infused intravenously with 3 million each of CD4 $^{+}$ and CD8 $^{+}$ T cells. T cells

expressed either no construct (non-transduced control) (n=5), or α -MOG synNotch- α -EphA2/IL13R α 2 CAR circuit (n=6). **(B and C)** Tumor size (B) and survival (C) were monitored over time. Tumor size was determined by bioluminescence imaging. Negative control treatment (non-transduced T cells) shown in grey, α -MOG SynNotch-CAR circuit treatment shown in pink. p<0.001 by t test with Holm-Sidak correction for multiple comparisons (on day 40). Thin lines show traces for individual animals; thick line shows geometric mean. See fig. S9G for analysis of off-target specificity (using non-brain implanted tumor). Survival was analyzed over 60 days by Log-rank (Mantel-Cox) test. p = 0.005. **(D)** GBM6 tumor-bearing mice were euthanized six days after α -MOG SynNotch-CAR T cell infusion. Representative confocal fluorescent microscopy of brain sections reveals that T cell mediated killing (cleaved caspase 3 staining) is restricted to the tumor. Scale bar, 2mm (left), 50 μ m (right). **(E)** Insets (single stained images) are enlargements of outlined regions in main images. Expression of cleaved caspase 3 is confined to the tumor cells (yellow) as indicated by white arrows in the overlay image. Scale bar, 20 μ m.

Supplemental Materials and Methods

Mass cytometry. 2-3 x 10⁶ T cells from each culture condition were washed two times in phosphate buffered saline (PBS, Fluidigm). Cells were resuspended in 5mL of PBS plus 5ul of cisplatin (Fluidigm Catalog: 201064), which was used to assess cell viability. After a 5 minute incubation at room temperature, the cisplatin reaction was quenched with 5 ml of cell staining media (CSM, 1X PBS with 0.05% bovine serum albumin and .02% sodium azide). Cells were washed twice in PBS and cells were then fixed with 1.6% paraformaldehyde in PBS for 10 minutes at room temperature, followed by two washes with 1X PBS. Samples were subsequently flash frozen on dry ice for further use. Upon thawing and washing in CSM, titrated amounts of each cell surface antibody were added to the sample for 30 minutes at room temperature. Cells were then washed twice with CSM and permeabilized by adding Perm-S buffer for 10 minutes on ice, followed by centrifugation. The cell pellet was re-suspended in Perm-S staining antibody cocktail and incubated for 30 minutes at room temperature. Following intracellular staining, sample was washed with 4 ml of Perm-S buffer followed by one wash with CSM. Finally, samples were resuspended in IR-intercalator (0.5uM iridium intercalator and 1% paraformaldehyde in 1X PBS), washed once with CSM and twice with ddH₂O, and filtered through a 50um cell strainer (Thermo Fisher). Cells were then resuspended at 1×10⁶ cells per mL in ddH₂O with 1x EQ four-element beads (Fluidigm Corporation, #201078). Cells were acquired on a Fluidigm Helios mass cytometer. per mL in ddH₂O with 1x EQ four-element beads (Fluidigm Corporation, #201078). Cells were acquired on a Fluidigm Helios mass cytometer.

Supplemental Figures

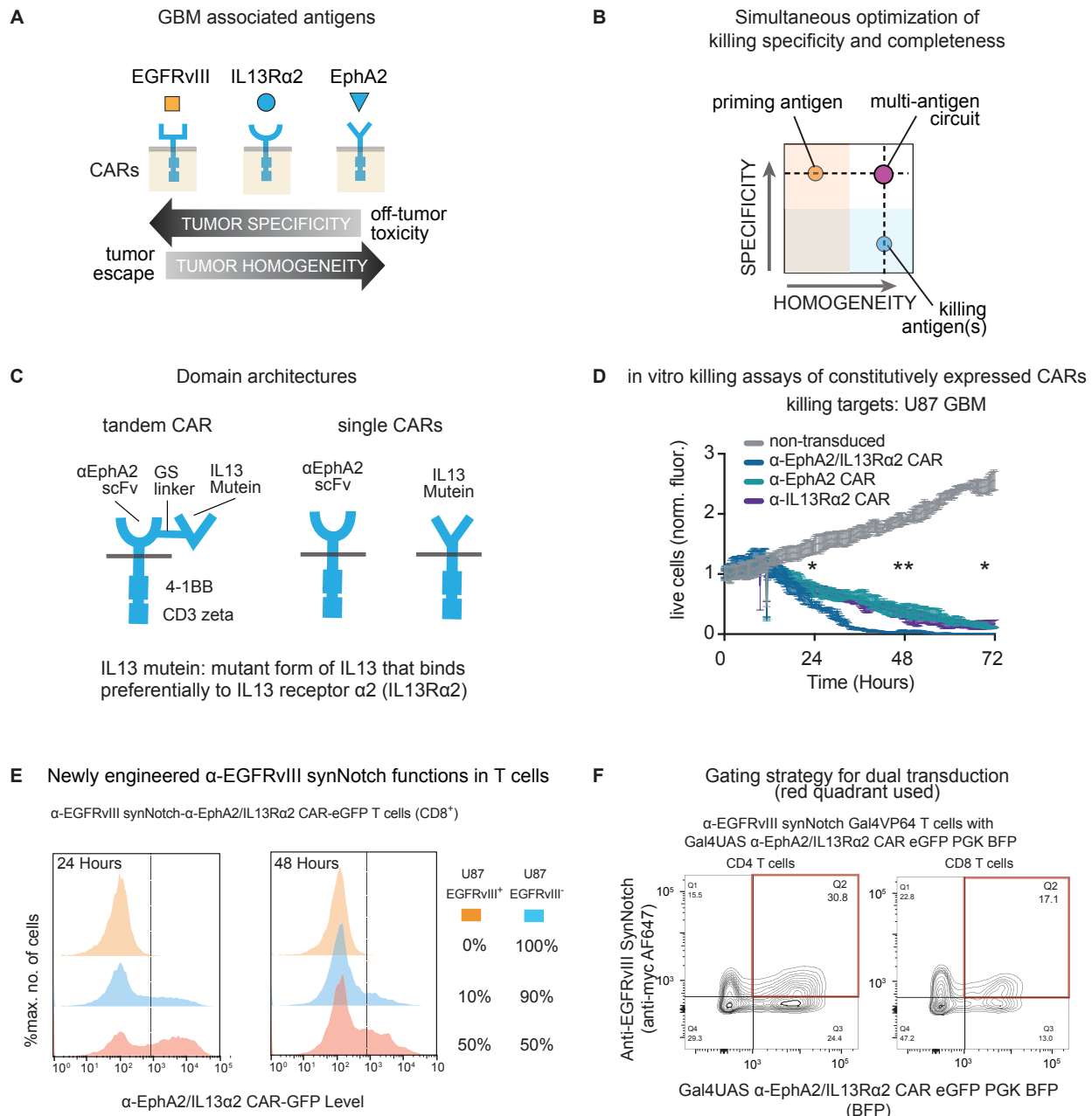


Fig. S1. Construction and testing of α-EGFRvIII synNotch-α-EphA2/IL13Ra2 CAR T cells against U87 GBM. (A) A diagram depicts the limitations of targeting GBM using single-antigen CAR T cells. Neoantigen EGFRvIII is tumor-specific, but heterogeneous, allowing tumor escape from α-EGFRvIII CAR T cell treatment (6, 11, 12). Conversely, other potential target antigens (EphA2 or IL13Ra2) are more homogeneously expressed in GBM, but also expressed in some normal tissues, leading to potential on-target, off-tumor toxicity. These dual challenges

limit the therapeutic window for CAR T cells. **(B)** The synNotch-CAR combinatorial antigen circuit harnesses the specificity of EGFRvIII combined with the homogeneous expression of the tandem killing antigens. **(C)** Domain architecture of α -EphA2/IL13R α 2 CAR, α -EphA2 CAR, and α -IL13R α 2 CAR. IL13 mutein is a mutant form of IL13 (E13K, K105R) that preferentially binds to IL13R α 2 (38). **(D)** Comparing killing of U87 wild-type cells (EphA2 $^+$ IL13R α 2 $^+$) by the α -EphA2/IL13R α 2 CAR versus T cells expressing either an α -EphA2 CAR or an α -IL13R α 2 CAR. Killing was measured using fluorescently labelled U87 cells in an IncuCyte killing assay measuring total fluorescence (live cells) over time (n=3, error bars are SEM). Statistical differences in killing were evaluated at 24, 48, and 72 hours by a one-way ANOVA followed by a Tukey's multiple comparisons test (all p-values were lower than 0.05). **(E)** Primary CD8 $^+$ synNotch CAR T cells were co-cultured with U87 cells as in Figure 1D. T cell priming after 24- or 48-hour exposure was measured by tracking induction of α -EphA2/IL13R α 2 CAR fused with a GFP reporter. Flow cytometry histograms show no induction of CAR expression in the absence of priming cells, and CAR induction with as low as 10% EGFRvIII $^+$ priming cells. Data are representative of at least 3 independent experiments. Dashed line delineates the positive population from the negative one. **(F)** Representative contour plots showing expression of the α -EGFRvIII synNotch Gal4VP64 receptor and the corresponding response elements regulating α -EphA2/IL13R α 2 CAR 4-1BB ζ CAR fused to green fluorescent protein (GFP) and constitutively expressing blue fluorescent protein (BFP) in primary CD4 $^+$ and CD8 $^+$ T cells. T cells positive for the synNotch receptor were stained through the myc-tag present on the synNotch receptor and the response element was selected based on BFP expression. The T cells in the red-boxed quadrant were sorted for in vitro and in vivo experiments.

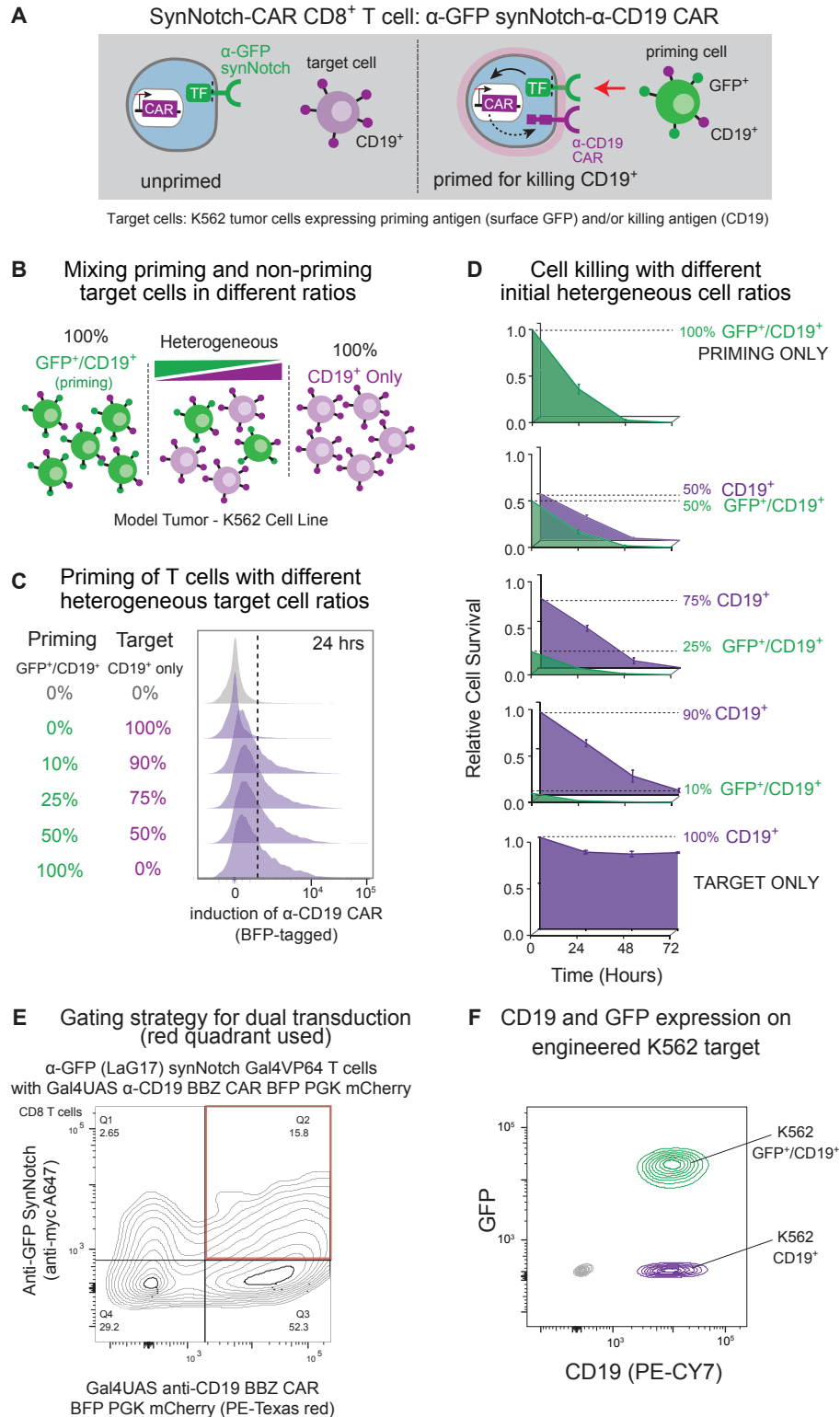
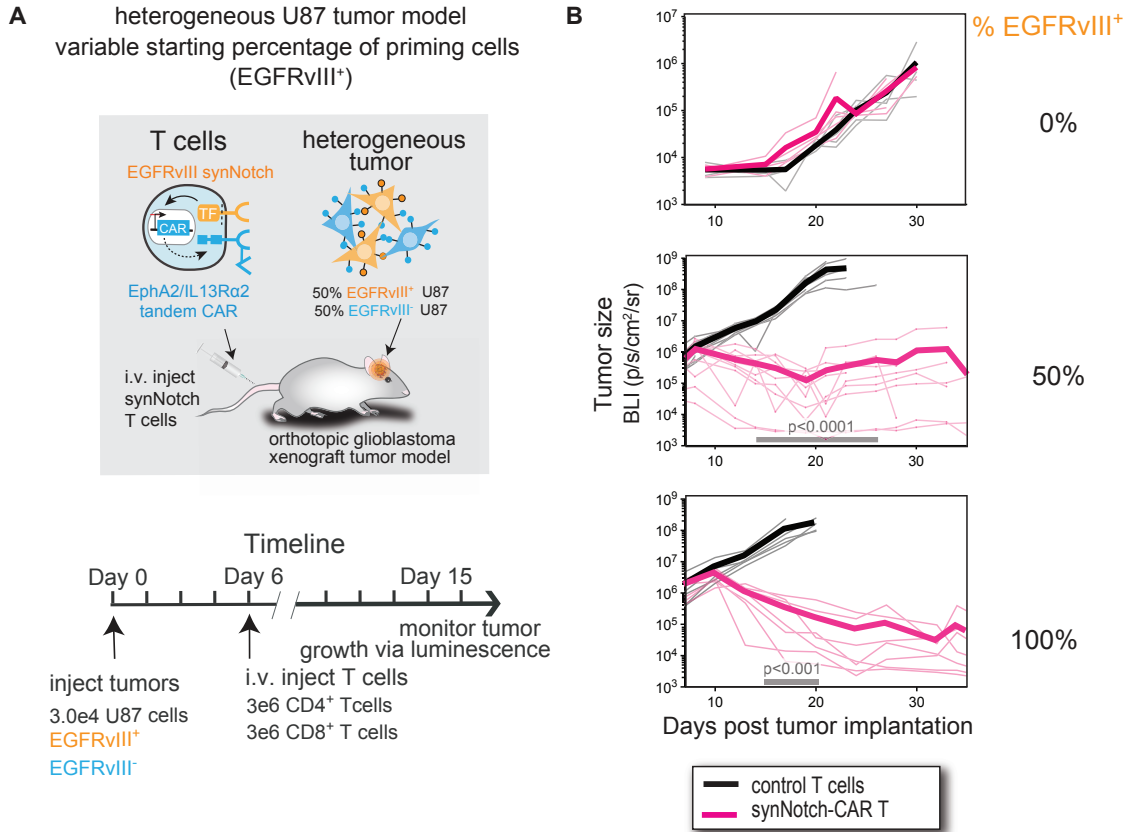


Fig. S2. Prime-and-kill circuit in T cells can overcome heterogeneity using a model antigen system in vitro. (A) Design of α -GFP (Lag-17) synNotch- α -CD19 4-1BB ζ CAR CD8⁺ T cells. synNotch-CAR T cells expressing this circuit are designed to ignore K562 target cells expressing

the killing antigen CD19 only (left) but kill cells that express both GFP and CD19 (right). **(B)** Tumor heterogeneity was recapitulated in vitro by mixing K562 priming cells ($\text{GFP}^+ \text{CD19}^+$) and target only cells (CD19^+) in different priming/target cell ratios (from 0-100%). **(C)** Primary human CD8 $^+$ T cells expressing the indicated synNotch-CAR circuit were co-cultured with the K562 mixtures and T cell priming was measured after 24 hours by tracking induction of CD19 CAR fused with a BFP reporter. Data are representative of at least 3 independent experiments. Dashed line delineates the positive population from the negative one. **(D)** Relative cell survival was quantified over 72 hours of synNotch-CAR T cell and target cell co-culture ($n=3$, error bars are SEM). **(E)** Representative contour plots showing expression of the α -GFP synNotch Gal4VP64 receptor and the corresponding response elements regulating α -CD19 4-1BB ζ CAR BFP PGK mCherry in primary CD4 $^+$ and CD8 $^+$ T cells. T cells positive for the synNotch receptor were stained through the myc-tag present on the synNotch receptor and the response element was selected based on mCherry expression. The T cells in the red-boxed quadrant were sorted and used for experiments in Figure 2. **(F)** Flow cytometry plots showing the expression level of CD19 and GFP on dual antigen K562s and CD19 on single antigen K562s utilized for in vitro experiments.



CONCLUSIONS: Tumor killing *in vivo* is only observed with 50 and 100% priming cells.

Fig. S3. α -EGFRvIII synNotch- α -EphA2/IL13Ra2 CAR T cells mediate effective and localized anti-tumor response against U87 GBM that heterogeneously express EGFRvIII in the brain. (A) U87 GBM cells were orthotopically implanted into immunodeficient NCG mice. Tumors contained one of the following three priming/target cell ratios: 100% U87 (EGFRvIII-negative) target tumor cells, 50%/50% of U87-EGFRvIII-positive (priming) and EGFRvIII-negative (target) tumor cells, or 100% U87-EGFRvIII-positive (priming) cells. Tumor cells were engineered to express luciferase to allow for tracking of tumor size. Six days following tumor implantation, the mice were infused intravenously (i.v.) with 3 million each of CD4⁺ and CD8⁺ T cells. T cells expressed either no construct (non-transduced control) or α -EGFRvIII synNotch- α -EphA2/IL13Ra2 CAR circuit. **(B)** Tumor size was determined by longitudinal bioluminescence imaging (BLI). Individual traces for each animal are shown with thin lines, while geometric mean is shown with the thick line. Negative control treatment with non-transduced T cells is shown in black, synNotch-CAR T cell treatment is shown in pink. n=10 animals per group for 50%/50% of U87-EGFRvIII-positive tumor model. p< 0.001 by Mann-Whitney test performed at

time-points day 12 to day 26 for synNotch-CAR vs non-transduced control T cells. For 100% U87-EGFRvIII-positive tumor model, n= 7 animals for synNotch-CAR T cell treatment group and n=6 for non-transduced control group. p<0.001 by Mann-Whitney test on day 13 onwards for synNotch-CAR vs non-transduced control T cells.

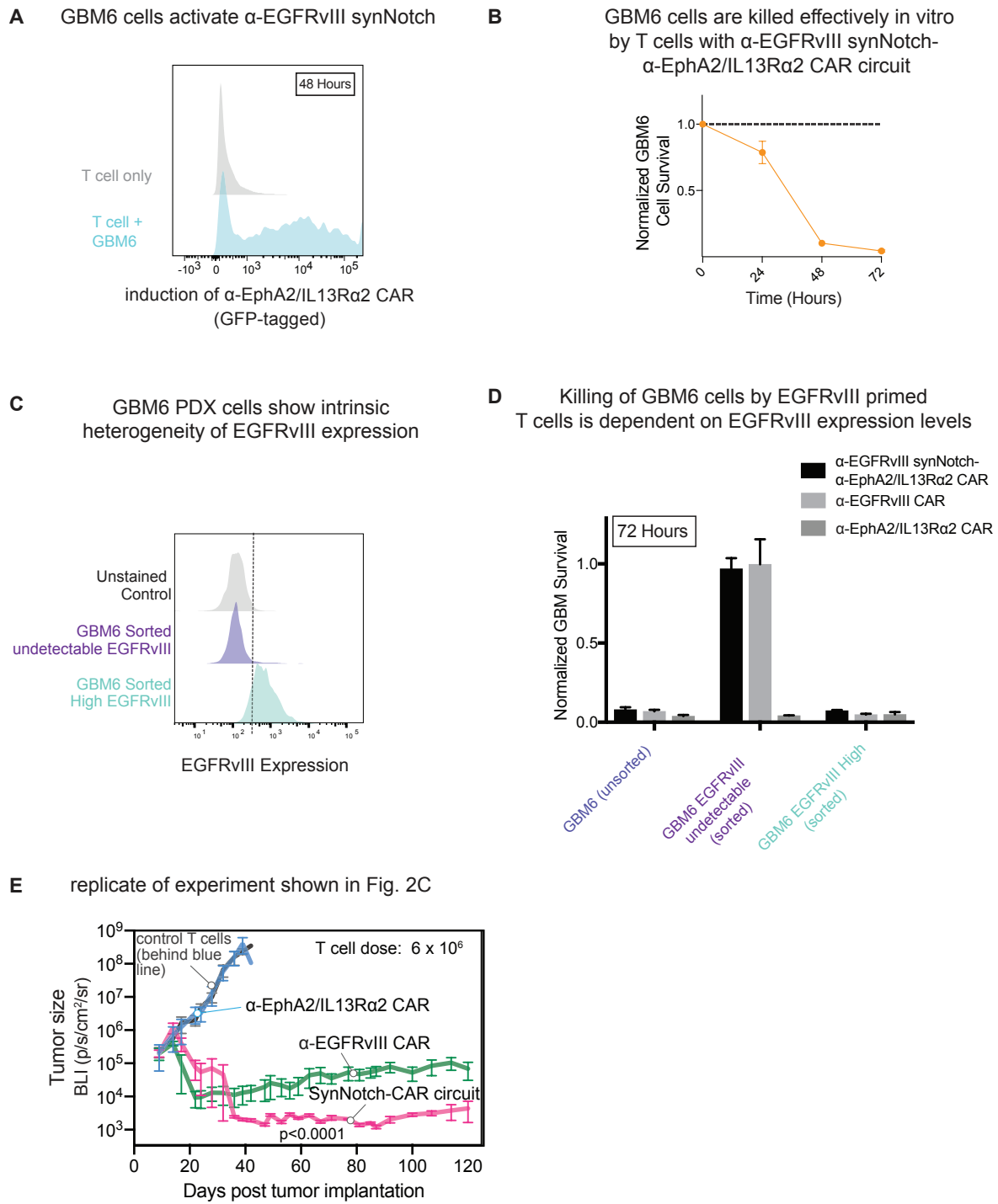
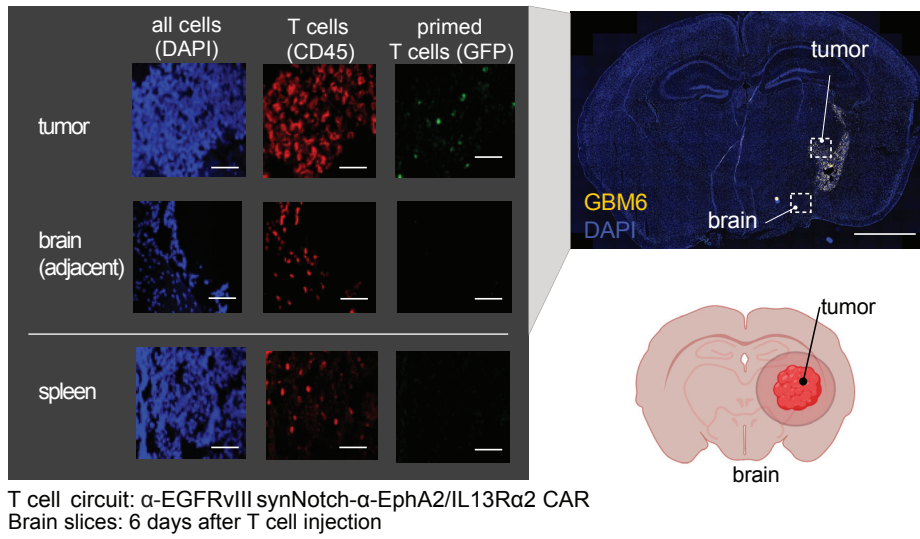


Fig. S4. α -EGFRvIII synNotch- α -EphA2/IL13Ra2 CAR T cells are effective against GBM6 tumor cells in vitro and in vivo. (A) Primary CD8⁺ α -EGFRvIII synNotch- α -EphA2/IL13Ra2 CAR T cells were co-cultured with or without GBM6 cells at 1:1 E:T ratio. T cell priming after 48-hour exposure was measured by tracking induction of α -EphA2/IL13Ra2 CAR fused with a GFP reporter. Flow cytometry histograms show no induction in the absence of GBM6 cells, and

significant induction with GBM6 cells (representative of at least 3 independent experiments). **(B)** Killing assays with primary CD8+ α -EGFRvIII synNotch- α -EphA2/IL13R α 2 CAR T cells with the circuit were co-cultured with GBM6 cells at 1:1 E:T ratio. Relative cell survival over 72 hours was quantified (n=3, error bars are SEM). **(C)** GBM6 cells were sorted for varying expression of EGFRvIII and evaluated by flow cytometry post-sort. Gray represents unstained control. Dashed line delineates the positive population from the negative one. **(D)** Killing assays with primary CD8⁺ α -EGFRvIII synNotch- α -EphA2/IL13R α 2 CAR T cells, α -EGFRvIII CAR T cells, or α -EphA2/IL13R α 2 CAR T cells co-cultured with sorted GBM6 cells expressing no EGFRvIII or high EGFRvIII or with unsorted GBM6 cells. Relative cell survival over 72 hours was quantified (n=3, error bars are SEM). **(E)** GBM6 cells engineered to express mCherry and luciferase were implanted orthotopically into the brains of NCG mice. Ten days following tumor implantation, mice were infused intravenously with 3 million each of CD4⁺ and CD8⁺ T cells. T cells expressed either no construct (control) (n=5), α -EGFRvIII synNotch- α -EphA2/IL13R α 2 CAR circuit (n=6), constitutively expressed α -EGFRvIII CAR (n=5), or constitutively expressed α -EphA2/IL13R α 2 tandem CAR (n=5). Tumor size was evaluated by longitudinal bioluminescence imaging. Negative control treatment with non-transduced T cells is shown in black (behind the blue line), synNotch-CAR T cell treatment is shown in pink (n=6), conventional α -EGFRvIII CAR T cell treatment is shown in green (n=6), and constitutive α -EphA2/IL13R α 2 tandem CAR T cell treatment is shown in blue (n=5). p< 0.0001 by t-test comparing non-transduced versus synNotch-CAR T cells. Error bars represent mean \pm SEM from one experiment.

A T cells are primed (GFP) and expand (higher numbers of red CD45+ cells) only within the GBM6 tumor. No primed T cells are observed in adjacent brain tissue (non-tumor) or in spleen



B visualization of T cells priming and killing within GBM6 tumor

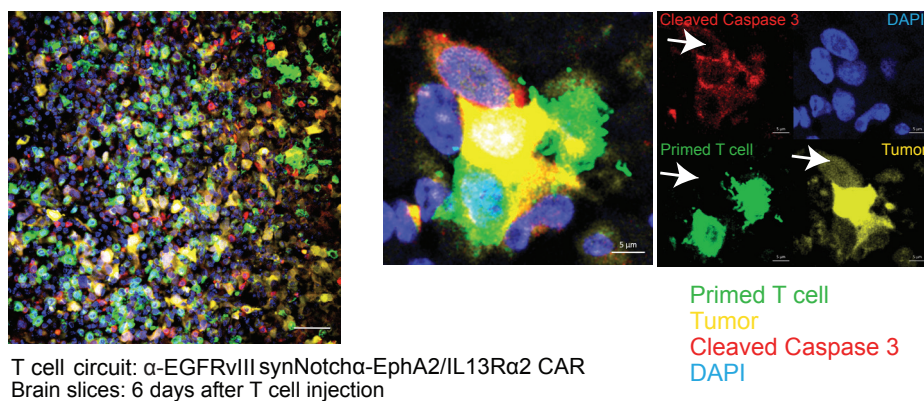
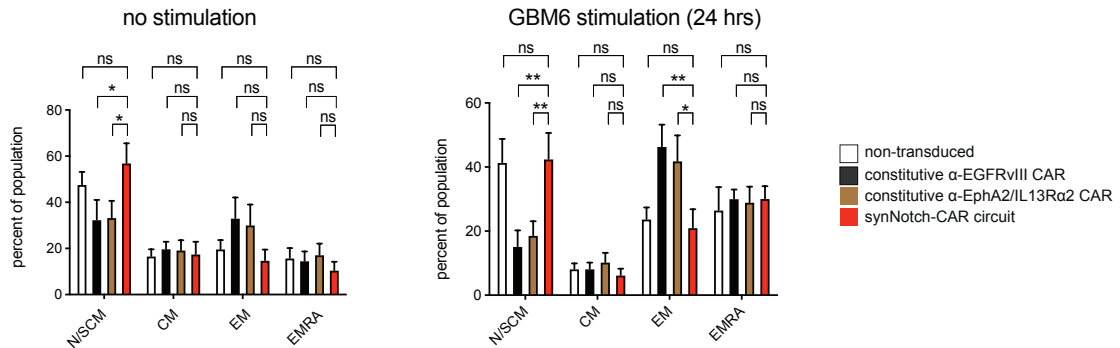


Fig. S5. Fluorescence imaging of brain slices from NCG mice with implanted GBM6 tumors treated with α-EGFRvIII synNotch-α-EphA2/IL13Ra2 CAR T cells. (A) GBM6 tumor-bearing mice were euthanized six days after α-EGFRvIII SynNotch-CAR circuit T cell infusion. Representative confocal fluorescent microscopy images of brain sections obtained from circuit T cell-treated mice reveals primed T cells (GFP⁺ indicates priming; red indicates human T cells identified with hCD45 staining) in the tumor (yellow). No primed T cells were observed in the adjacent brain tissue or spleen. Insets (single stained images, scale bar: 50μm) are enlargements of outlined regions in the main image (Scale bar: 1mm). **(B)** Confocal fluorescent image of tumor core showing robust infiltration and interaction of GFP⁺ primed synNotch CAR T cells in close proximity to a GBM6 tumor cell (yellow). Cleaved Caspase 3 staining (in red)

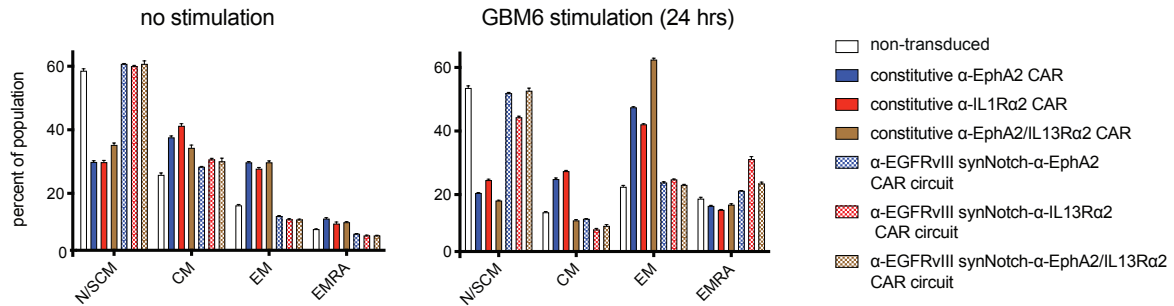
shows colocalization with an apoptotic tumor cells. Right panel scale bar: 50um. Left panel:
Scale bar: 5um.

A T cell phenotype distribution: constitutive CARs vs SynNotch induced CAR circuit (cells used in Fig. 3C and 5B)



CONCLUSION: synNotch-CAR circuit yields higher level of naive/stem central memory phenotype than either constitutive CAR, both with and without target cell (GBM6) stimulation

B T cell phenotype distribution: Comparison of 3 Constitutive CARs vs. SynNotch-induced versions (cells used in Fig. 5C)



CONCLUSION: All α-EGFRvIII synNotch-induced CAR circuits (stippled bars) consistently yields higher level of naive/stem central memory phenotype compared to the constitutively expressed CARs (solid bars), either with or without GBM6 target cell stimulation

C α-EGFRvIII synNotch-α-EGFRvIII CAR circuit also shows more naïve-like phenotype

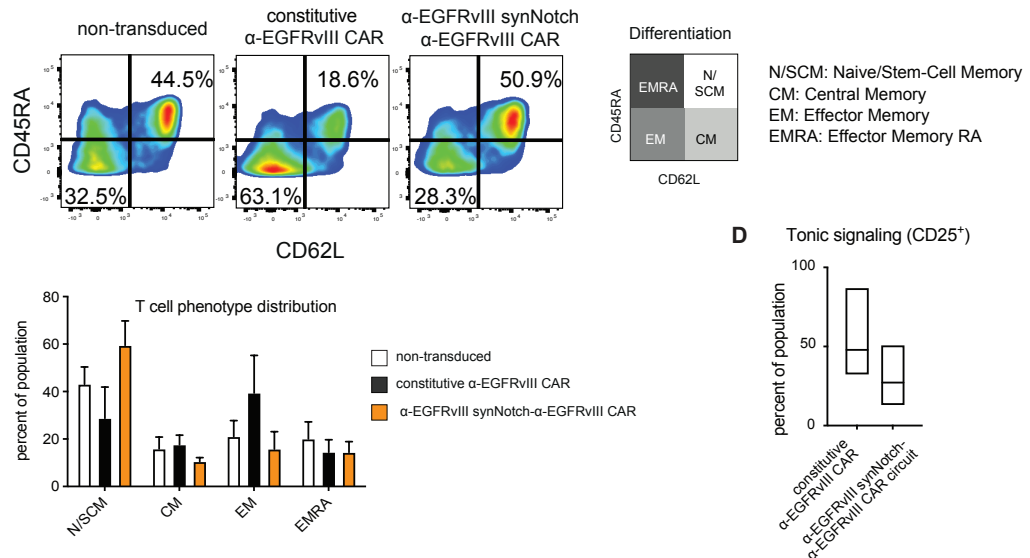
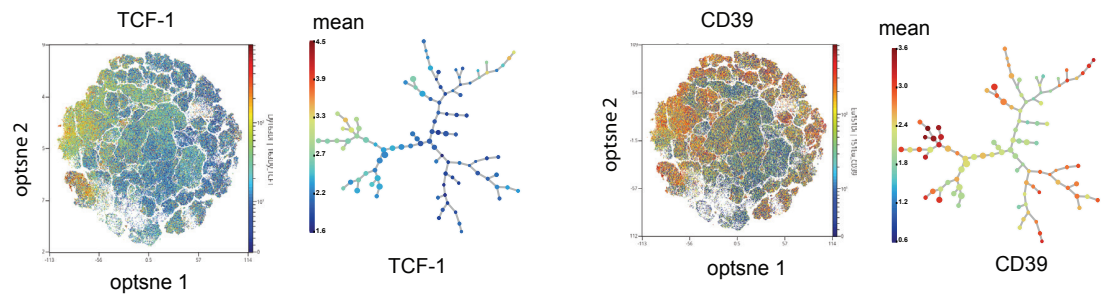


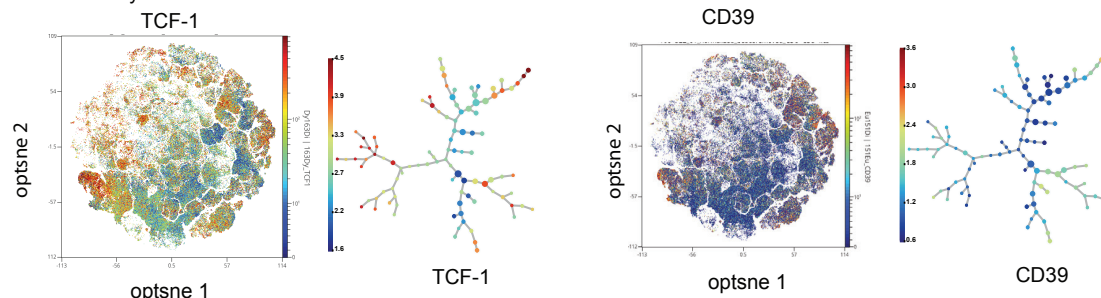
Fig. S6. SynNotch-CAR T cells show more naïve-like phenotype compared to comparable

constitutively expressed CAR T cells. **(A)** Surface expression of CD45RA and CD62L was used to distinguish naïve-like cells (N/SCM; CD45RA⁺CD62L⁺), central memory cells (CM; CD45RA⁻CD62L⁺), effector memory cells (EM; CD45RA⁻CD62L⁻), and effector memory RA cells (EMRA; CD45RA⁺CD62L⁻). Cell phenotype distribution for non-transduced T cells compared with T cells bearing constitutive α-EGFRvIII CAR, constitutive α-EphA2/IL13Ra2 tandem CAR, or synNotch-CAR circuit. T cells were analyzed without (left panel) or with 24 hour stimulation with target GBM6 cells (right panel). Error bars represent mean ± SEM of 6 donors. Data were analyzed by a two-way ANOVA followed by Dunnett's multiple comparison test. * = p < 0.05, ** = p < 0.01. **(B)** Full phenotypic analysis of the percentage of T cells in each indicated differentiation state assessed by surface expression as described in (A). Bars show the percent of T cell population with the corresponding phenotype (n = 3). T cells were analyzed without (left panel) or with 24 hour stimulation with target GBM6 cells (right panel). **(C)** Cell phenotype distribution for non-transduced T cells compared with T cells bearing constitutive α-EGFRvIII CAR, or α-EGFRvIII synNotch-α-EGFRvIII CAR circuit. The percentages of cells in the naïve/memory stem cell state and effector memory state are highlighted. The bar plot represents the average percentage of the different populations. Error bars represent mean ± SEM of 3 donors. **(D)** Tonic signaling of constitutive vs synNotch-induced α-EGFRvIII CAR T cells assayed by percent CD25⁺ population (n = 5 different donors). Boxes represent min to max with median center line.

A constitutive tandem CAR (EphA2/IL13Ra2)

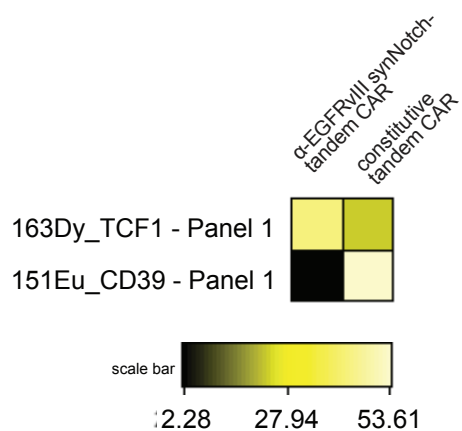


α -EGFRvIII synNotch tandem CAR circuit



CyTOF analysis of constitutive tandem CAR and α -EGFRvIII synNotch tandem CAR T cells after in vitro expansion. All single, viable CD3 $^+$ CD8 $^+$ T cells were subjected to non-linear dimension reduction algorithm opt-SNE for visualization in 2D space. TCF1 and CD39 expression overlaid on opt-SNE embedding (color indicates marker expression intensity). Data was clustered using FlowSOM and visualized by minimum spanning tree with color indicating mean expression intensity.

B

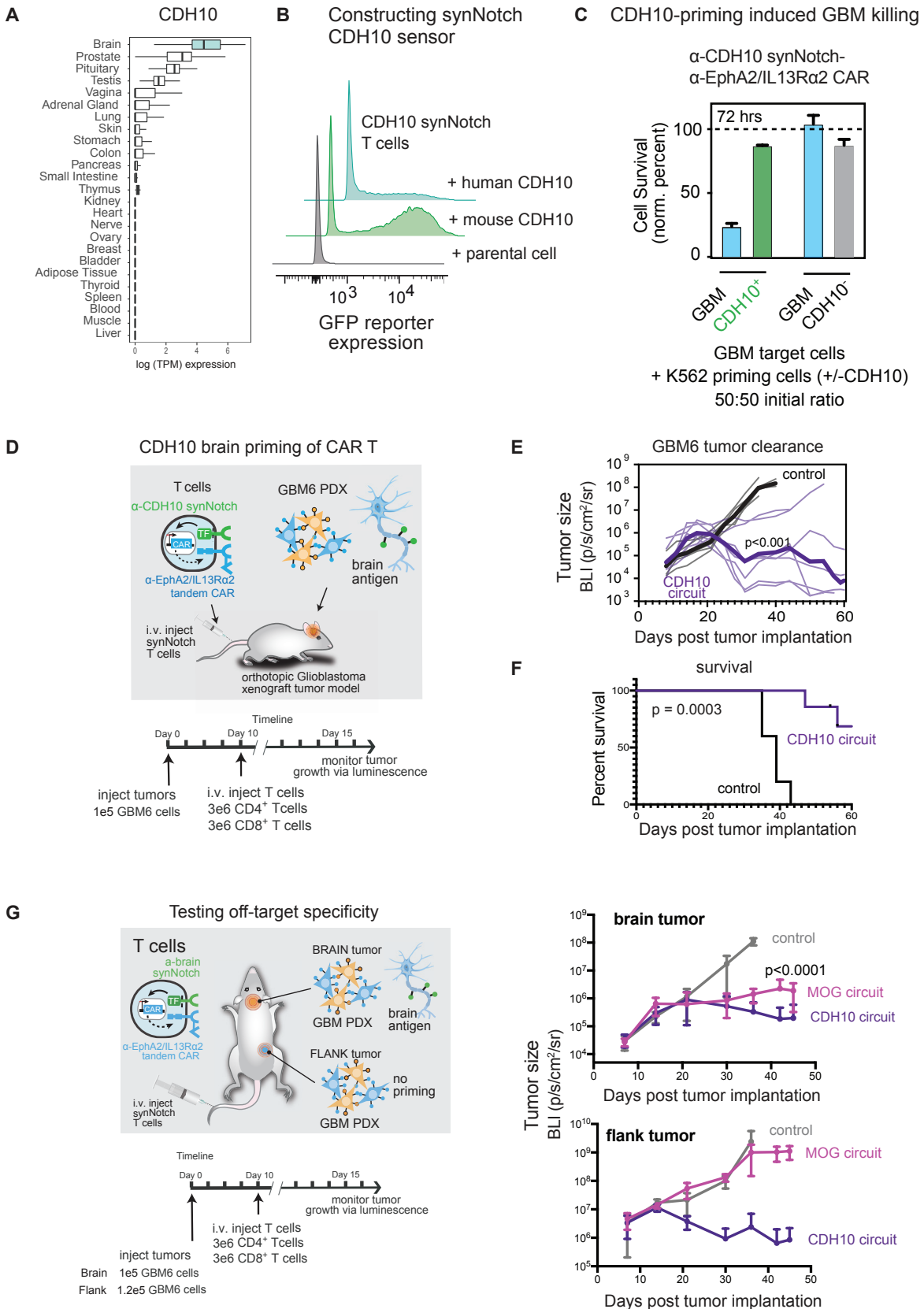


Heatmap showing expression of CD39 and TCF1 on α -EGFRvIII synNotch tandem CAR and constitutive tandem CAR $^+$ T cells (color indicates marker expression intensity).

Fig. S7. Mass cytometry shows that synNotch-induced circuits yield T cells with increased expression of stemness marker TCF1 and reduced expression of exhaustion marker CD39.

(A) Expression of TCF1 and CD39 on constitutive tandem CAR (EphA2/IL13Ra2) and α -EGFRvIII synNotch- α -EphA2/IL13Ra2 CAR T cells after in vitro expansion. Single, viable CD3 $^+$ CD8 $^+$ T cells were subjected to the non-linear dimension reduction algorithm opt-SNE

for visualization in 2D space. TCF1 and CD39 expression overlaid on opt-SNE embedding (Left Panels; color indicates marker expression intensity). Data were also clustered using FlowSOM and visualized by minimum spanning tree with color indicating mean expression intensity (Right Panels). **(B)** Heatmap showing expression of CD39 and TCF1 on α -EGFRvIII synNotch- α -EphA2/IL13R α 2 CAR and constitutive α -EphA2/IL13R α 2 CAR T cells (color indicates marker expression intensity).



CONCLUSIONS: α -MOG synNotch is a more precise brain priming receptor than α -CDH10 synNotch.

Fig. S8. Construction and testing of α -CDH10 synNotch- α -EphA2/IL13R α 2 CAR T cells.

(A) Box and whisker plots showing tissue specific expression of CDH10 across a subset of tissue samples in GTEx v7. Units shown are log-scaled normalized RNAseq counts (Transcripts Per Million) taken from GTEx portal v7 (<https://gtexportal.org/>). **(B)** Primary CD8 $^{+}$ α -CDH10 synNotch-GFP PGK BFP T cells were co-cultured with either parental K562 or K562 transduced to express mouse CDH10 or human CDH10. T cell priming after 48-hour exposure was measured by induction of GFP reporter expression. Data are representative of 3 experiments. **(C)** Primary CD8 $^{+}$ α -CDH10 synNotch- α -EphA2/IL13R α 2 CAR T cells were co-cultured with U87 cells and K562 expressing or not expressing mouse CDH10. Relative cell survival over 72 hours was quantified and showed cytotoxic capacity of α -CDH10 synNotch- α -EphA2/IL13R α 2 CAR T cells to kill U87 cells only when priming cells are expressing mouse CDH10 (n=3, error bars are SD). Significant cytotoxicity in the U87 co-cultured with K562 mouse CDH10 was observed (**p < 0.001; t test) compared to the U87 co-cultured with K562 Parental. Cell population ratio: 1:1:1, 1x10⁴ cells each. **(D)** Immunodeficient NCG mice were orthotopically implanted in the brain with mCherry- and luciferase-expressing GBM6 patient-derived xenograft cells. Ten days following tumor implantation, the mice were infused intravenously with 3 million each of CD4 $^{+}$ and CD8 $^{+}$ T cells. T cells expressed either no construct (non-transduced control) or α -CDH10 synNotch- α -EphA2/IL13R α 2 CAR circuit (n=7). **(E and F)** Tumor size (E) and survival (F) over time. Tumor size was determined by longitudinal bioluminescence imaging. Negative control treatment with non-transduced T cells is shown in grey, synNotch-CAR T cells treatment is shown in purple. Individual traces for each animal are shown with thin lines, while geometric mean is shown with the thick line. p<0.001 by t test with Holm-Sidak correction for multiple comparisons (E), p = 0.0003 Log-rank (Mantel-Cox) test (F). **(G)** GBM6 PDX tumor cells were implanted in the brain and flank of NCG mice. Both tumors express the killing antigens (EphA2 and IL13R α 2), but the expression of priming antigen, MOG or CDH10, is restricted to the brain. Mice were treated one-time (10 days after tumor implantation) with intravenous infusion of non-transduced (n=5) T cells, α -MOG-synNotch-CAR T cells (n=6), or α -CDH10-synNotch-CAR T cells (n=5). Tumor size was measured by bioluminescence. α -MOG-synNotch-CAR T cells are shown in pink, α -CDH10-synNotch-CAR T cells are shown in purple while the non-transduced control T cells are shown in gray. p < 0.0001; t test MOG synNotch-CAR T cells vs non-transduced control T cells.

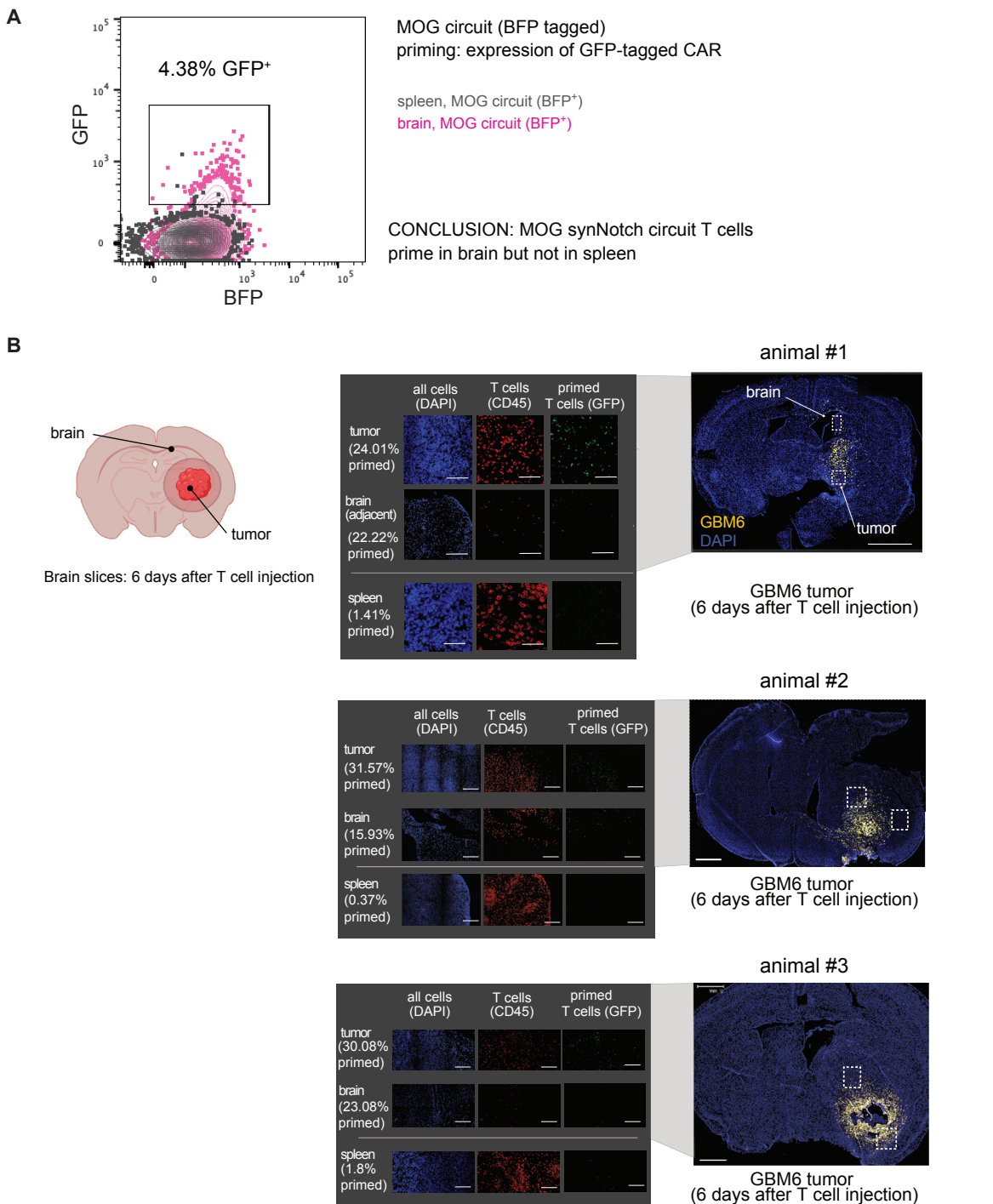
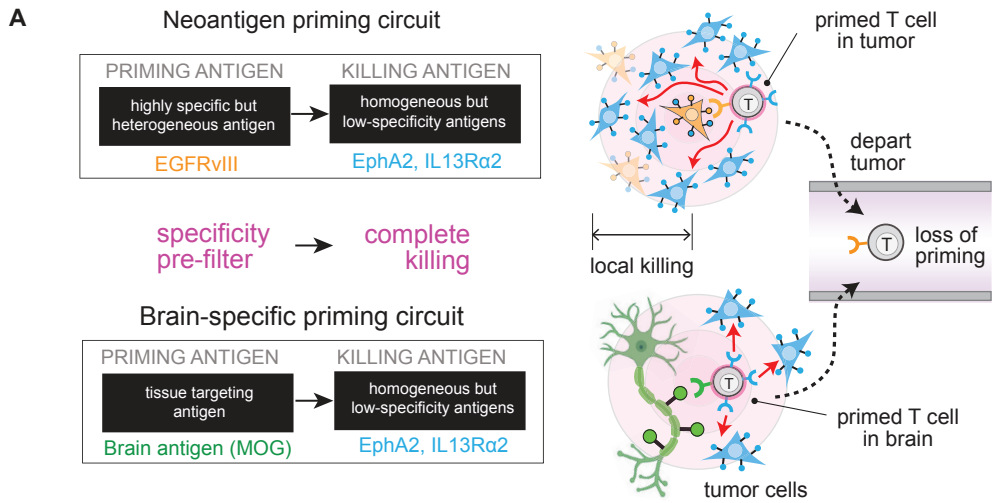


Fig. S9. Brain-specific synNotch-CAR T cells mediate effective anti-GBM responses. (A) Flow cytometry of α -MOG synNotch CAR T cells isolated from brain and spleen of GBM6-bearing mouse demonstrates presence of GFP⁺ primed T cells in the brain but not in the spleen. SynNotch CAR T cells express BFP constitutively. T cells were pre-gated on CD3 and CD45. **(B)** GBM6 tumor-bearing mice were euthanized six days after α -MOG SynNotch-CAR circuit T

cell infusion. Representative confocal fluorescent microscopy of brain sections obtained from circuit T cell-treated mice reveals primed T cells (GFP^+ indicates priming; red indicates human T cells identified with hCD45 stain) in the tumor (yellow) and in adjacent parts of the tumor. Quantification of GFP^+ T cells in the tumor using nuclear segmentation reveals greater number of GFP^+ T cells in tumor core than in the periphery (percentage of GFP^+ primed T cells is shown on the left side of the image panels). Circuit CAR T cells (red) in the spleen do not express GFP. Scale bar, 1mm. Insets (single stained images, scale bar: 50 μm) are enlargements of outlined regions in the main image.



B Advantages of prime-and-kill multi-antigen circuits

- TUMOR SPECIFICITY**
 - Multi-antigen recognition yields significantly higher specificity
 - Prevents off-tumor toxicity
 - Can utilize normal tissue-specific antigens as part of recognition signature
- COMPLETENESS OF KILLING**
 - Insensitive to heterogeneity of priming antigens
 - High homogeneity of killing antigen(s) sufficient for complete killing
- POTENCY/PERSISTENCE**
 - Induced CAR expression maintains greater fraction of naive-like T cells
 - Reduced exhaustion, increased *in vivo* persistence

Fig. S10. Strategies for design of synNotch-CAR T cells to treat glioblastoma. (A) synNotch-CAR circuits combine advantageous features of multiple individually imperfect antigens to achieve far better therapeutic recognition of tumor cells. A priming antigen (either neoepitope or tissue-specific antigen) can be used to achieve precise killing, even if the priming antigen is heterogeneously expressed or expressed on non-cancer cells within the CNS. A homogeneous killing antigen (or combination of antigens) can then be subsequently targeted to achieve complete tumor killing. Priming antigens can lead to more complete killing because they can induce T cells to execute trans-killing of multiple neighboring cells bearing the CAR antigens. This primed killing is spatially restricted to the tumor, even if killing antigens are expressed elsewhere, because once the T cells depart the region, the lack of priming signals leads to rapid loss of CAR expression. (B) Multi-antigen prime-and-kill circuits can achieve much improved tumor-specific targeting by recognizing multi-antigen signatures that could incorporate antigens expressed on different cells within the tumor (including heterogeneous malignant cells, or non-

malignant cells), thereby reducing off-tumor toxicity. At the same time, even though they increase the precision of tumor recognition, these circuits still allow for more complete killing of tumor cells. The T cells are insensitive to heterogeneity or partial loss of priming antigen, and completeness of killing can be achieved as long as the killing antigen (or antigens) have high homogeneity. Finally, we also find that synNotch-CAR T cells are more naive-like and more persistent than their equivalent constitutively expressed CAR T cells, leading to far more effective and durable tumor clearance *in vivo*. These features could make synNotch-CAR T cells very useful for targeting diverse solid cancers that present similar challenges to GBM.

Movies S1-S2

Movie S1. Real-time killing assays using different heterogeneous mixtures of EGFRvIII⁺ and EGFRvIII⁻ target cells show efficient trans-killing. Time-lapse analysis of 50,000 synNotch-CAR T cells co-cultured with mixtures of EGFRvIII⁺ and EGFRvIII⁻ tumor cells. EGFRvIII⁺ and EGFRvIII⁻ U87 cells were mixed at 100% and 0%, 90% and 10%, or 50% and 50%, respectively, for a total of 10,000 U87 cells. EGFRvIII-positive priming cells are colored in yellow and EGFRvIII-negative target cells are colored in blue. T cells are unlabeled. Fluorescent images were obtained every 15 minutes over 3 days using an IncuCyte Live-Cell Imaging System.

Movie S2. Intravital imaging of circuit CAR T cells show dynamic priming within the GBM6 xenograft tumor. Tumors were implanted at a depth of 3mm below the right frontal cortex and cranial windows were implanted. Tumor cells are shown in orange, unprimed synNotch-CAR T cells are shown in blue, and primed CAR-expressing synNotch-CAR T cells are shown in green.

Data File S1. Raw Data. Provided as a separate excel file.